2017-08-01

Crack Healing in 304L Stainless Steel Using Additive Manufacturing and Friction Stir Processing (FSP)

Cameron Scott Gygi
Brigham Young University

Crack Healing in 304L Stainless Steel Using Additive Manufacturing (AM) and Friction Stir Processing (FSP)

Cameron Scott Gygi

A thesis submitted to the faculty of
Brigham Young University
in partial fulfillment of the requirements for the degree of

Master of Science

Michael P. Miles, Chair
Tracy W. Nelson
Yuri Hovanski

School of Technology

Brigham Young University

ABSTRACT

Crack Healing in 304L Stainless Steel Using
Additive Manufacturing (AM) and Friction
Stir Processing (FSP)

Cameron Scott Gygi
School of Technology, BYU
Master of Science

Continuing an investigation on using FSP to heal stress corrosion cracks (SCC) in welds on nuclear reactors, this study seeks to use AM in addition to FSP to aid crack repair.

Previous studies address that current repair technology on nuclear reactors involves the use of TIG welding which can allow helium atoms to aggregate and form voids at the grain boundaries. This weakens the material and renders the repair ineffective. Another previous study evaluated the effectiveness of FSP alone in repairing SCC which did have defects depending on the parameters used during FSP. This study evaluated the use of AM in addition to FSP.

Literature is available on FSP and AM separately and literature is available on technologies that used both them together. However, the current processes that are available that use both AM and FSP can be expensive and may be impractical for some purposes. This study shows a new process that is both less expensive and more practical in SCC repair.

Initial proof of concept trials was performed on 1018 mild steel using both wire fed additive and insert additive technologies. A slot would be removed and filled in with an additive process and processed using FSP. Because of poor repeatability, substantial distortion, and voids present this study went forward using insert technologies in further experiments rather than wire wed additive technologies. In addition, the depth and width of the insert or area where the added material would be placed was varied in initial trails.

Tensile testing was performed on initial steel trials and the stainless steel experiments and it demonstrated a correlation between depth of the added material and the tensile strength. Micro-hardness mapping performed on initial steel trials also showed hardening in the FSP stir zone

Three-point bend tests were performed to show that an existing crack underneath the FSP zone would not propagate through the nugget. All evaluations supported a substantial increase in yield strength increased after FSP.

Keywords: Cameron Gygi, friction stir processing, additive manufacturing, arc welding, stainless steel, tensile testing, micro-hardness mapping, crack healing, 304L

ACKNOWLEDGEMENTS

I would like to thank Dr. Miles for the guidance and expertise given during this project. I would not be where I am today without him. I would like to also thank The National Science Foundation and Brigham University for without the support and use of equipment this project would not have been possible. I would also like to thank Dr. Nelson and Dr. Hovanski for their additional expertise and help with moving this project forward.

I would additionally like to thank Janel Mayfield, Cameron Gunter, Eliza Snyder, Tyler Hampton, Nolan Crook, Scott Taysom, Shane Wood, Kevin Shirley, TJ Barton, and Jameson Marriot for the help and support given to help me with this project. Their help and experience helped this research project move more smoothly. Finally, I would like to thank my wife, Ansley Gygi, who supported me continuously during this project along with my two sons Jacob and Isaac.

TABLE OF CONTENTS

LIST OF TABLES

LIST OF FIGURES

1 INTRODUCTION

1.1 Background

Because FSP is process that has seen a lot of development and innovation, a substantial amount of literature is available. Literature ranges from tool optimization to micro-structural evaluations of processed specimens. Recently more literature is becoming available on using FSP and AM together because of the advantages of a hybrid process. FSP has been widely used to refine grain structures in stainless steels and do crack repair in stainless steel welds. However, when combined with an additive process it usually uses a powder fed system that can be expensive and in some cases not very practical.

1.1.1 Crack Repair Using Arc Welding or FSP

Products made primarily of steel and stainless steel can face stress corrosion cracking while in service especially in the nuclear industry. Stress corrosion cracking (SCC) is a prominent occurrence especially under continual or prolonged use of the product. Depending on severity of the crack many solutions are available for repair through conventional welding methods such as gas metal arc welding (GMAW). When products develop cracks while in service, and conventional welding methods cannot be used, replacement may be the best option currently available. In some cases, that may be very expensive or there may not be a safe way to dispose of the product such as spent nuclear fuel. Additionally, arc welding puts a large amount

of energy into the weld which then allows helium to become an interstitial atom and create voids along the grain boundary. Conventional welding techniques usually require high heat and a filler metal that closely matches the alloy of the base material. While traditional welding can be done with no filler metal, healing a crack without any filler can put additional stress on the part after a weld due to shrinkage of the weld nugget from cooling. Volume reduction is a common occurrence in welds with no filler material. Trapped oxides in a crack can result in poor metallurgical bonding and eventual part failure. This may cause the weld to crack again, which in turn requires further repair. In cases where filler metal is not needed, Friction stir welding or friction stir processing (FSW or FSP) is a good option. This is because it produces no fumes and can refine the grains below the austenite temperature (Razmpoosh, 2015). With grain refinement, yield strength, and fracture toughness increase. Crack healing may be difficult if the crack is too large or too deep. Furthermore, since the base material does not reach the melting temperature, the crack can be healed without helium entering the weld (Lin, 1990).

1.1.2 Wire Fed Additive Manufacturing

Wire fed additive manufacturing has recently made several improvements and extensive research is being done so that it can be put to use in industry. This is because AM can help create geometries that cannot be machined. Also software technology has made wire fed AM manufacturing easier to automate and easier to prototype new designs. Because the wire fed AM technology uses technology similar to GMAW to deposit the metal, the resolution between print layers is poor but further research is being done to improve in this area (Razmpoosh, 2015).

There is a possibility that the combined use of GMAW and FSP may be able to overcome the issues faced with crack healing. A crack would be machined out to expose virgin material

and remove oxides. Then the opening is filled using GMAW or another metal additive process to replace and add extra material. Finally, the filled section would be processed by FSP to blend the material together and reduce grain size. Internal stresses caused by the added material could be reduced because the grains will undergo recrystallization as part of the FSP. The process could increase the hardness of the material and reduce void content or barriers due to bead deposits from GMAW alone. (Razmpoosh, 2015).

1.2 Purpose of the Research

The purpose of this research is to evaluate FSP and AM used together to heal SCC.

1.3 Research Hypotheses

This project will be using a GMAW welder or machined inserts to fill cut out areas or open slots in steel plates and then use FSP to process the added material. Previous work using FSP alone in crack repair often had micro-voids in the cross section of the stir zone (SZ) on the pin. With that in mind:

H1: Using added material in an area requiring repair, full consolidation between the base material and added material will occur when using proper FSP parameters.

H2: If an existing crack is beneath the surface it will not propagate through the stir zone when a stress is applied, as simulated by three-point bend testing.

1.4 Delimitations

This study will be performed on 1018 steel for proof of concept trials and then 304L because of its abundant use in nuclear applications. It will also be performed on non-irradiated metal

because this work will be supportive work for future studies on irradiated material. The tool used in this study is Polycrystalline Cubic Boron Nitride-Tungsten-Rhenium (PCBN-W-RE) hybrid because of its effectiveness in FSP of steels and stainless steels. A GMAW (Gas Metal Arc Welding welder) welder will be used along with machined inserts as a wire fed AM technology.

1.5 Definition of Abbreviations and Terms

Advancing / Retreating Side (AS, RS)-in FSP the advancing side is the side of the tool where the rotational motion is in line with the traversing direction. The retreating side is the opposite side.

ASTM-American Society for Testing Materials; standards used for specimen dimensions and testing

Base Material-Material that has not been processed since coming from the mill.

Bead-On-Plate-and FSP run on a plate, no joining of other plates occurs.

CNC-Computer Numerical Control

Dogbone-specimens used for tensile testing

EDM-Electrical Discharge Machining

FSP-Friction Stir Processing

GMAW-Gas Metal Arc Welding.

GTAW-Gas Tungsten Arc Welding

TIG-Tungsten Inert Gas

MIG-Metal Inert Gas.

HAZ-Heat Affected Zone-area between FSP nugget and base material.

IPM-Inches Per Minute-traveling speed of FSP tool.

PCBN-W-Re-Polycrystalline Cubic Boron Nitride; A hybrid material used for FSP in this project.

Q70-Designation used by Megastir for a tool made from 70% PCBN and 30% W-Re.

RPM-Revolutions Per Minute.

SCC-Stress Corrosion Cracks/Cracking.

Stir Zone (SZ) / Weld Nugget- Processed material by the FSP tool.

Traversing-Lateral movement of FSP tool.

Tunnel Defect-pin hole that runs along the length of the AS of the SZ.

Z-Force-Applied downward force during FSP.

Square end mill: Machining tool that has a square cutting profile.

Ball nose end mill: Machining tool that has a round cutting profile.

2 LITERATURE REVIEW

2.1 Introduction

Literature on FSP by itself and wire fed metal AM are available to form a solid foundation of understanding of both technologies. Additional review was done on GMAW because of the similarities between GMAW and continuous wire fed AM technologies.

2.2 Friction Stir Welding and Processing

Because the purpose of this research is to investigate the effects of FSP on material that has been added to a component, literature on friction stir welding and processing was reviewed and evaluated. While FSP has proven very successful in aluminum, more work is being done to improve its ability to process steel and stainless steels (Reynolds, 2003). This is because steel is a much more difficult material to process because of its high temperature flow stress and low thermal diffusivity (Reynolds, 2003). FSP has a finer grain size than many arc welding applications. This is because with most arc welding applications you melt the base material. When solidification occurs, grain size can increase depending on the cooling rate. With FSP you are not melting the base material, but using the tool to get the metal to forming temperatures which will refine the grains. Therefore, in FSP the grains are much smaller than what you would find in a MIG weld. This can be seen in figure 4-13 and 4-14. FSP has its own advantages from FSW. FSP gives you more control over the processed zone and it has active heating and cooling. It is also more energy efficient than conventional welding methods. It also has significant

advantages in joining dissimilar materials such as carbon steels to aluminums. It has been advantageous in joining exotics and aerospace materials. FSP is a solid-state processing technique with one step processing that achieves microstructural refinement, densification, and homogeneity (Reynolds, 2003). The microstructure and mechanical properties of the processed zone can be accurately controlled by optimizing the tool design. Most conventional welding/joining processes are difficult or cannot have depth control changes while welding. Some literature as shown FSP joints that have successfully bonded metal with ceramic material to improve strength and hardness. A ceramic metal composite material has desired mechanical properties, but they can be lost when the material goes under heat treatment or arc welding (Mishra, 2003) (Mahmoud, 2010). The material could have a higher strength and hardness but lacks toughness. FSP can be used to process specific areas in the material to join or increase strength and hardness and yet leave other areas to have higher toughness. What makes this process advantageous for this project is that with the added material that will be blended with the base material, we will get a complete homogeneous mix and a stronger metallurgical bond. Because it's a solid state process it would it also help to preserve existing desirable mechanical properties (Nagaoka, 2015) (Razmpoosh, 2015) (Park, 2003).

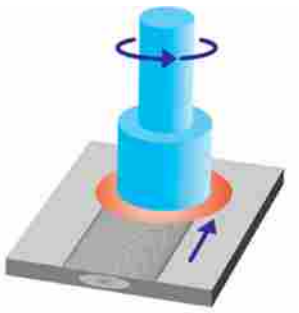

Figure 2-1: Friction Stir Processing Schematic

Different parameters like rotational velocity measured in rotations per minute (RPM), Z force, or traversing speed can vary and affect mechanical strength, yield strength and hardness of the weld. The principle behind FSP is frictional heat created by a rotating tool that is plunged into the base material as shown in figure 2-1. The heat from the friction causes the metal to plasticize or become malleable. This is because welding or processing is done below the melting temperature. The plasticization allows the metal to be blended and pushed together in order to form a bond. For applications in welding steel, harder materials need to be used such as polycrystalline cubic boron nitride (PCBN) or Q70 (70% PCBN / 30% W-Re) tools. The tool used in this project can be seen in figure 2-2. This tool has an 8mm-long, threaded conical pin and a 25mm diameter convex shoulder.

Figure 2-2: Q70 Friction Stir Processing Tool

Distortion is often observed when welding because of the force required to plunge into the material. Although in comparison to other welding techniques FSP is preferable because it

has minimal distortion. Distortion can be mitigated with proper tooling and plate fixtures (Reynolds, 2003) (Grewal, 2014).

2.3 Additive Manufacturing

Currently there are three main methods in metal additive manufacturing. The first and the most common is Direct Metal Laser Sintering (DMLS). This process uses a high powered laser to sinter the powder and bond layers of material. Generally, layer thickness or resolution can range from 3 to 40 microns of thickness. This process has shown promising results in producing difficult geometry and in printing materials that cannot be fabricated by traditional methods (Gåård, 2006). Improvements are being made with build quality by improving the surface of prints by changing layer thickness of the powder being deposited. A more homogeneous microstructure was achieved by using a higher power laser with a lower scanning speed (Fino, 2013). Another method that is growing in popularity is wire fed metal AM. This method is based upon technology from GMAW or MIG. This method also uses a laser to form a molten pool. The wire is then fed into that pool and then the wire feeding head traverses to create a pattern or layer based on a CAD model. This method forms a strong metallurgical bond because the substrate is melted along with the wire. Parts produced from this process have shown high tensile strengths and varying hardness depending on wire speeds and traversing speeds. However, it should be noted that the variance is less than ten percent (Ding, 2015). This method has grown in popularity because it is less expensive to produce metal wire for the printer which makes obtaining resources and operating the printer more economical. Wire fed metal additive manufacturing has poor surface finish and often parts are evaluated based on surface roughness. Printing efficiency is also poor and so attempts have been made to improve efficiency by using

combination printers. Combination printers utilize both wire fed technology and powder. This has helped improve efficiency but further work still needs to be done (Gåård, 2006).

2.4 Combination Friction Stir Processing and Additive Manufacturing Methods.

Though the process described in this project is new, other processes have been developed that combine the technologies in some way. One process demonstrated the ability to add powder to a groove and then process the material using friction stir processing. Experiments were done in aluminum and custom machinery was developed that could deposit powder and then FSP to blend the materials together. The research was focused on aluminum alloys but the processed can be used for steel (Mahmoud, 2010). This project would hope to develop an additional combination process that could also be used for many different metals and alloys. Additionally, it is desired to develop a process that is practical, low cost yet effective in corrosion crack repair.

2.5 Gas Metal Arc Welding (GMAW)

Further literature on wire fed additive methods show that it's a proven technology because of the extensive research work done on GMAW. GMAW can now be an automated process and yield very effective results. For the purposes of this work, we will be using a robotic and a manual MIG welder because of the speed at which it can fill in holes, and the lack of complexity of the geometry that would need to be created to fill in machined out areas. Investigation in the automation systems of MIG welding showed advances in locating systems, and improving overall quality of the work from the robotic welder. Some programing was done to facilitate needs such as varying Z height while welding, and to be able to weld multiple layers at one time. Coding was done on a PLC controller or teach pendant robot using G-code and existing functions. (Ding, 2015) (Clocksin, 1985).

Figure 2-3: Robotic MIG Welder

3 METHODOLOGY

3.1 Machining and MIG welding

Experiments were accomplished using a manual and robotic MIG welder, CNC machine, and a FSP machine already available at Megastir and at BYU. Trials were performed on 1018 mild steel for proof of concept, and then 304L stainless steel. A four inch by three quarter inch by two-foot plate was machined flat, using a CNC machine to remove the mill scale, and

Figure 3-1: Plate with Filled Slots

marked places for cutting. The marked places were used to identify slots and give width, length and depth dimensions. The slots were then cut to the proper size and depth using an end mill. Six different geometries were chosen so that experimentation could be done to see if any variation with depth and width would have effects on the process. Widths measuring 0.25” and 0.5” were chosen with varying depths of 0.25”, 0.375”, and 0.5”. This allowed six different geometries that would allow the ability to find any relationship or coloration. Once the slots were machined, they

were then filled in by the MIG welder robot (which can be seen in figure 3-1) or manual MIG. Though the slots in the plates were machined to varying sizes, settings on the welder remained the same to keep consistency. This allowed each slot to be completely filled with mild steel filler wire. Settings used to fill the slot were 21 volts at 210 inches per minute. Once the slots in the plate were filled, the plate was then faced flat again to prepare for FSP to prevent damage to the tool. Figure 3-2 shows a 1018 steel plate that has been filled and is about to be resurfaced. The MIG welds had a higher hardness than the base material and the slots had to be filled above the top to ensure complete filling. Because of the factors of higher hardness and sudden rise in material, care was taken to prevent tool damage. A sudden change in depth could damage the insert and so the plates were re-machined to be flat again before FSP. Changes were made to the slot geometry by using a ball nose end mill in some experiments rather than using a square end mill, an explanation for the change is given in the results section. Eventually experiments were also run on plates that had machined inserts instead of MIG filled areas. Inserts were machined to match the dimensions of the machined slot in the plate and then the insert was placed in the slot. With a machined insert the plate did not have to be resurfaced. Care had to be taken to ensure the slot depth and insert thickness were the same to prevent height changes. Height changes could cause potential issues with FSP especially when using force control. The tool may adjust to a shallower depth to keep the same z force if the insert is slightly taller than the slot wall. When moving to experimentation with stainless steel, the inserts had to be tack welded down using GTAW.

Figure 3-2: Machining Slots

When experiments were performed using 304L stainless steel, a few changes had to be made to the procedure to protect the tool and to achieve optimal performance during the welds. FSP passes were run on plates with no inserts to find parameters that would work and then performed on plates with inserts. Because each plate was processed with three FSP passes, one experiment was done with different pass orders to see if there was any variation in the results of the final weld if the passes occurred in different order. Also the thickness of plate that was chosen for

304L was 0.5” instead of 0.75”. This was done to allow for comparison with previous stainless steel crack healing experiments (Gunter, 2016).

3.2 Friction Stir Processing

Using a PCBN tool, the plate was processed using the FSP machine. All experiments were done using a Q70 tool shown in figure 2-2. Experiments conducted used 100RPM, 3IPM, and Z force of 12,000-12,500 pounds for 1018 steel. After proper parameters were identified 200 RPM, 3 IPM, and a Z force of 10,000 pounds were used for 304L stainless. Once the plate was processed, places were identified and cut for sample observation. These markings corresponded to the areas where the slots were located. Cross sections revealed that one pass was not enough to blend all the material together especially in areas that had wider slots. To ensure complete blending three passes were done. One pass directly down the center of the plate and a pass 0.25” to the left and to the right. This was changed when microscopy showed that there was slight gap between the SZ of the second and third passes. The distance was then changed to 0.15” Pass order was originally starting the firth pass down the center. Then the second would go to the left and the third to right.

3.3 Microscopy

Specimens were cut perpendicularly or transversely across the FSP zone and mounted in bakelite that was heated. Some specimens that were wider than 1.25” had to be mounted in epoxy inside a 2” PVC ring. Specimens were then sanded to 1200 grit and diamond polished to 1 micron using an automated sanding and polishing machine. Once sanding and polishing had been completed the specimens were then prepared for microscopy in an etching solution. Etching was

done on steel specimens using a Nitol acid solution using 97 milliliters of methanol and 3 milliliters of nitric acid applied to the polished surface for 15 seconds. Stainless steel specimens were electro-etched using an oxcylic acid solution with an applied 7 volts for 45 seconds. A standard power supply was used along with a tungsten cathode and steel anode. The solution is made with 10 grams of oxcylic powder and 100 milliliters of distilled water.

Figure 3-3: Image of Stainless Steel Plate with 0.25” X 0.2” Insert at 7X

Views of the entire specimen were used for micrographs. While pictures taken at a higher magnification were used to measure grain size and identify phases and micro voids. Figure 3-3 shows a stainless steel experiment using a 0.25” X 0.2” insert. A macro void can be seen on the pin on the advancing side. This image however shows how blending of the insert would occur.

3.4 Tensile Testing

Some specimens cut from the welds were used for tensile testing. Specimens from a plate that did not undergo FSP and specimens from a plate that was MIG welded and FSP were used

for comparison purposes. This gave a before and after evaluation of the effects of FSP on repaired welds. Specimens that were prepared for tensile testing were cut using a band saw, or water jet. Specimens cut on the band saw had to be then placed on a custom made fixture seen in figure 3-4 and a CNC program was written to cut the reduced section of the dog-bone geometry.

Figure 3-4: Custom Fixture for Machine Dog-bones

The cutting process chosen depended material availability. Three dog bones were taken from each section to help identify trends. Specimens were then machined into dog-bones that were 101.6mm long and had a reduced section that was 31.75mm long. The top of the SZ was machined flat to remove any areas that could create a crack. Then the dog bone was flipped over and machined from the back side until it had a height of 6.35mm. This gave all the dog-bones a reduced cross section that was 6.35mm in height and in width. A drawing of the dog bones can be seen in figure 3-5. Specimens were then placed in an 50,000 N tensile machine. Specimens were pulled until failure at .16mm/sec and then the data was recorded and evaluated.

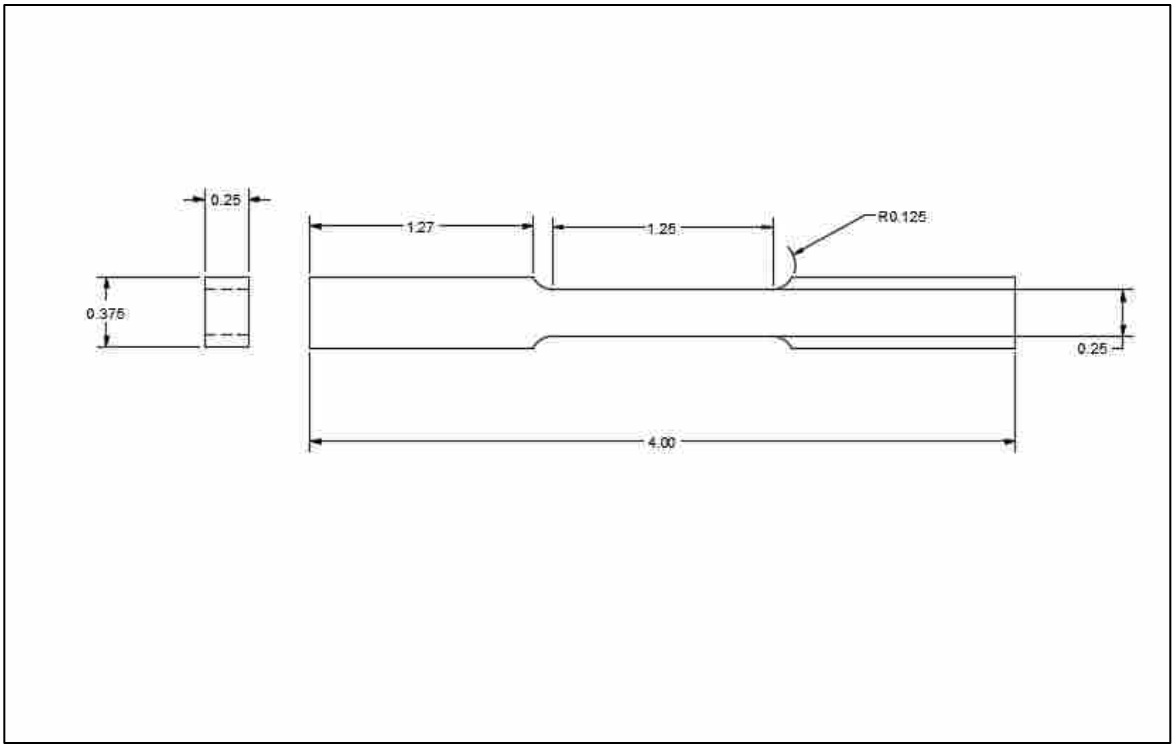

Figure 3-5: ASTM Mini Dog-bone

3.5 Micro-Hardness Mapping

Previously mounted specimens for microscopy were placed on a micro-hardness mapping machine. A grid was created using software on the micro-hardness mapping equipment. Each point on the grid was placed 400 microns apart and then a 10X lens would focus on each point on the sample. Then a diamond tool would go in and indent that same point. Once all the indents were performed then a 50X lens would focus on each point. The resulting size of the indent could then be used to calculate hardness in that area. The entire process took three days for each sample. The micro-hardness apparatus can be seen below in figure 3-6.

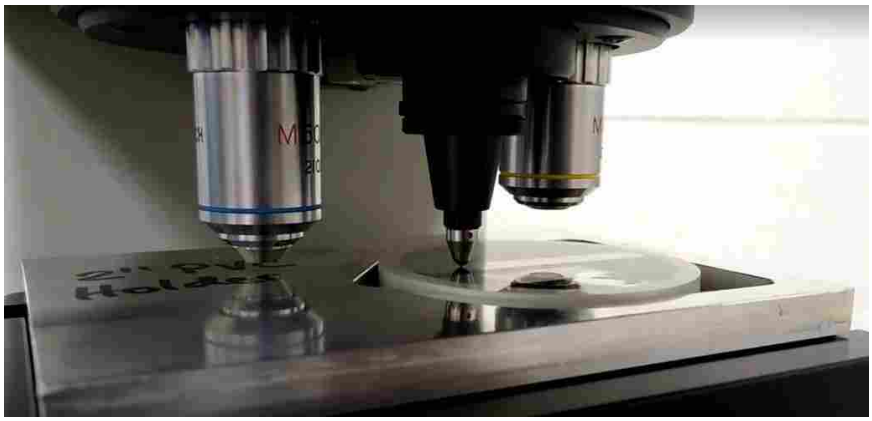

Figure 3-6: Micro-Hardness Set Up

3.6 Three Point Bend Testing

In order to simulate crack healing and crack propagation, three-point bend specimens were machined to proper size and then a crack was cut on the bottom side of the specimen using a wire EDM. The size of the specimen used was ASTM E8 three point-bend sample being 4 inches wide and 0.5” wide and 0.5” thick as shown in figure 3-7. The crack was machined using a wire electrical discharge machine (wire EDM) to cut a narrow notch design which can be found in the reference section. (Barrata, 1992). A fixture using three steel rods as the three points was used for experiments. Once the specimen was oriented correctly in the fixture, a load was applied to the center of the specimen until the top point had descended 0.3”. Once the test was completed specimens were cut in the transverse direction or perpendicular to the weld in half. One half was polished and etched and the crack was evaluated under the microscope.

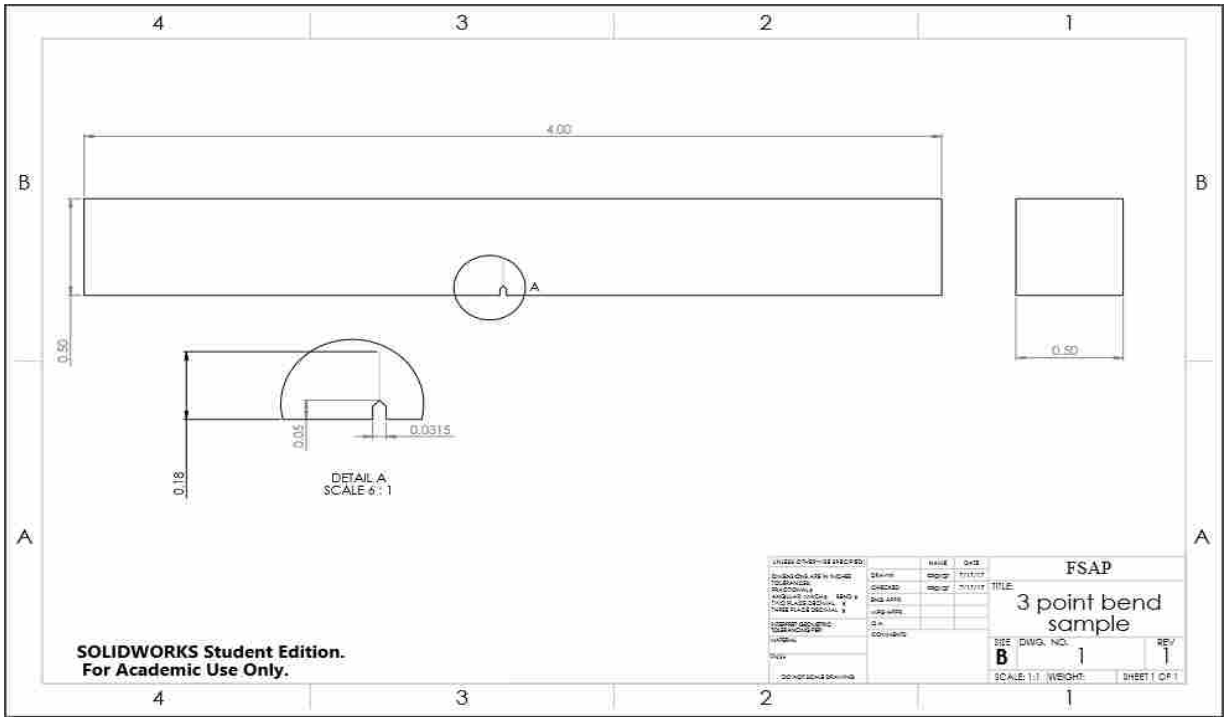

Figure 3-7: Three-Point Bend Specimen Drawing

4 RESULTS AND DISCUSSION

4.1 Microscopy

Specimens were taken after each experiment for microscopy. To observe any visible void content and determine the effectiveness of FSP in blending the added material. Specimens were first taken from a plate that did not undergo FSP. Each specimen was approximately 1" in length, 0.5" in height, and 0.07" or 2mm in thickness. Because there were six different geometries in the plate, six specimens were taken and mounted in bakelite. After the specimens were mounted, they were then prepared by sanding them to 1200 fine grit and then polished using diamond paste to one micron. Finally, the specimens were etched in 3% nitric acid and 97% methanol solution, otherwise known as 3% nitol. This further removed visible scratches and revealed the grain structure. Pictures were then taken under the microscope and documented. When specimens from the second experiment were prepared in the same manner, it was clear that one pass with the FSP tool was not sufficient enough to blend all the material. To correct this, three passes were used to ensure more complete blending. Results from the third experiment proved that three passes were effective and yielded improved results. This can be seen in figures 4-17 and 4-18. 4-17 shows a single slot of 0.25" X 0.375" filled by MIG welding and 4-18 shows a single pass over the area. Even though the tool was zeroed properly on the machine it still missed the MIG weld. This was more of a problem on welds that had a width of 0.5" because complete blending did not occur. With three passes total blending would occur and FSP was

assured to cover the entire targeted area. This improvement can be seen in figures 4-18 and 4-19. The second experiment also revealed large voids were consistent through all specimens. Because of the geometry of the square end mill, each slot had sharp corners at the bottom. This created a problem when the plate had to be filled because all experiments used the same MIG parameters for comparison. The voltage may have been too low to melt the corners and create sufficient wet out in larger geometries which would have yielded less voids. However, increasing the voltage did not guarantee complete void reduction and further increased the observed warping. It was decided that better results might come from an improved geometry design that would be more effective for lower or higher voltages. Using a ball nose end mill, this created a geometry that would allow the weld metal to pool and achieve sufficient wet out and further reduce void content even at a lower voltage. Upon using the ball nose in the third experiment, it was observed that much lower void content was achieved. The differences in microscopy can be seen in figure 4-1 with the square end mill geometry at the top and the ball nose at the bottom. The same slot width and depth dimensions were used but the ball nose geometry had significantly improved weld quality. In addition to void reduction, an increase in UTS and elongation was also observed because of improved weld quality. Because some voids were still observed in the larger geometries, a switch was made to using inserts instead of wire fed additive processes. This was done because of the significant distortion from the GMAW process and FSP. Machined inserts were placed into the slots in further experiments. This reduced void content completely and reduced set up time. Initially FSP passes were 0.25” inches apart. However, this changed to be 0.15” inches apart to decrease the space between subsequent passes and reduce any gaps between the pin from each SZ. When experiments were done on stainless steel, the same process was used to mount the specimens but a different etching solution was needed. Oxcylic acid was made

using 100 milliliters of distilled water and 10 grams of oxcylic powder mixed together. Each specimen was then placed into the acid and then an electrode was place on the specimen to electrochemically etch it and reveal the grain structure. Figure 4-2 shows the results after FSP parameters were adjusted to 200 RPM and 3 IPM using 8000 pounds of z force for stainless steel. No voids occurred on the advancing side and some the insert can still be seen because the oxide from the insert remains. However, a non-volumetric defect occurred that was only revealed when tensile specimens from were pulled, and failed in the SZ. Based on poor tensile data and elongation, another experiment was conducted using 100 RPM and 3 IPM. Previous stainless steel experiments using 100 RPM and 3 IPM had a tunneling defect and the tool broke during FSP. However, this experiment used no backward tilt and the depth the pin would plunge to was 0.2” inches. This experiment would use a 1° backward tilt and a plunge depth of 0.18” inches. Results can be seen in figure 4-3 which did achieve weld consolidation with the exception of a small void occurring on the advancing side. This void however had no effect on tensile strength.

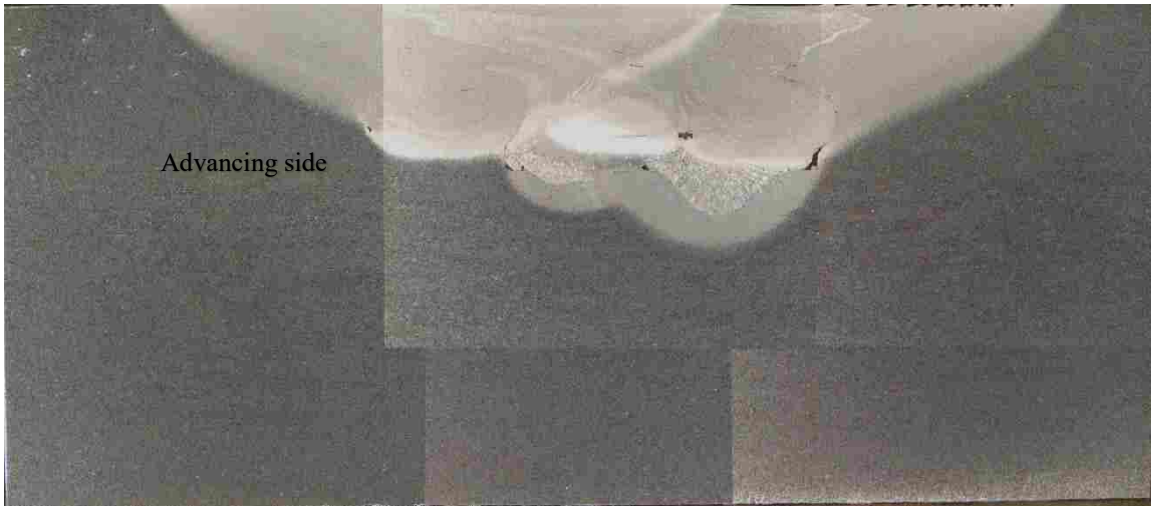

Figure 4-1: Square Geometry for 0.5” X 0.25”

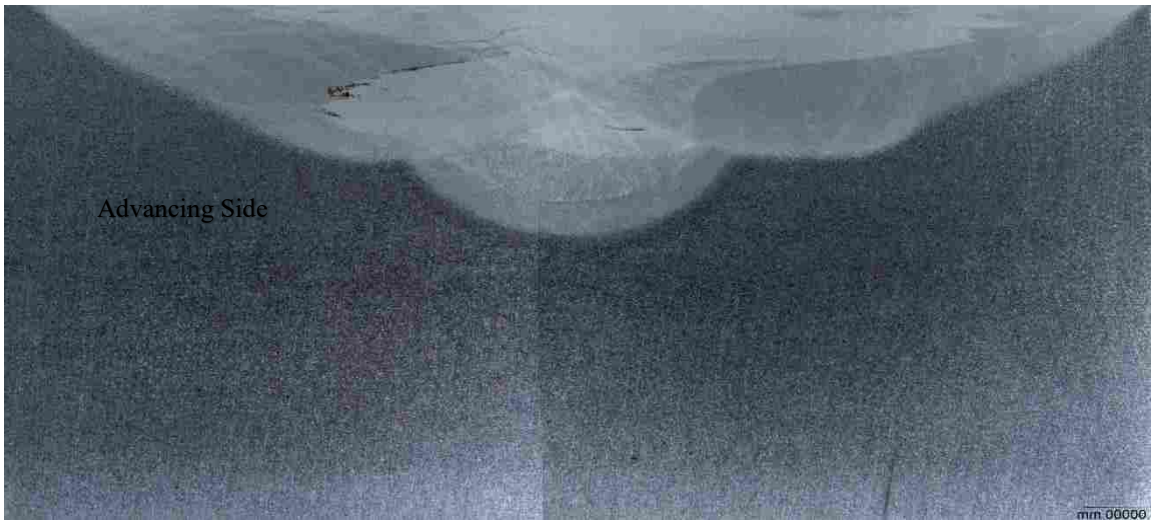

Figure 4-2: Ball-nose Geometry for 0.5” X 0.25”

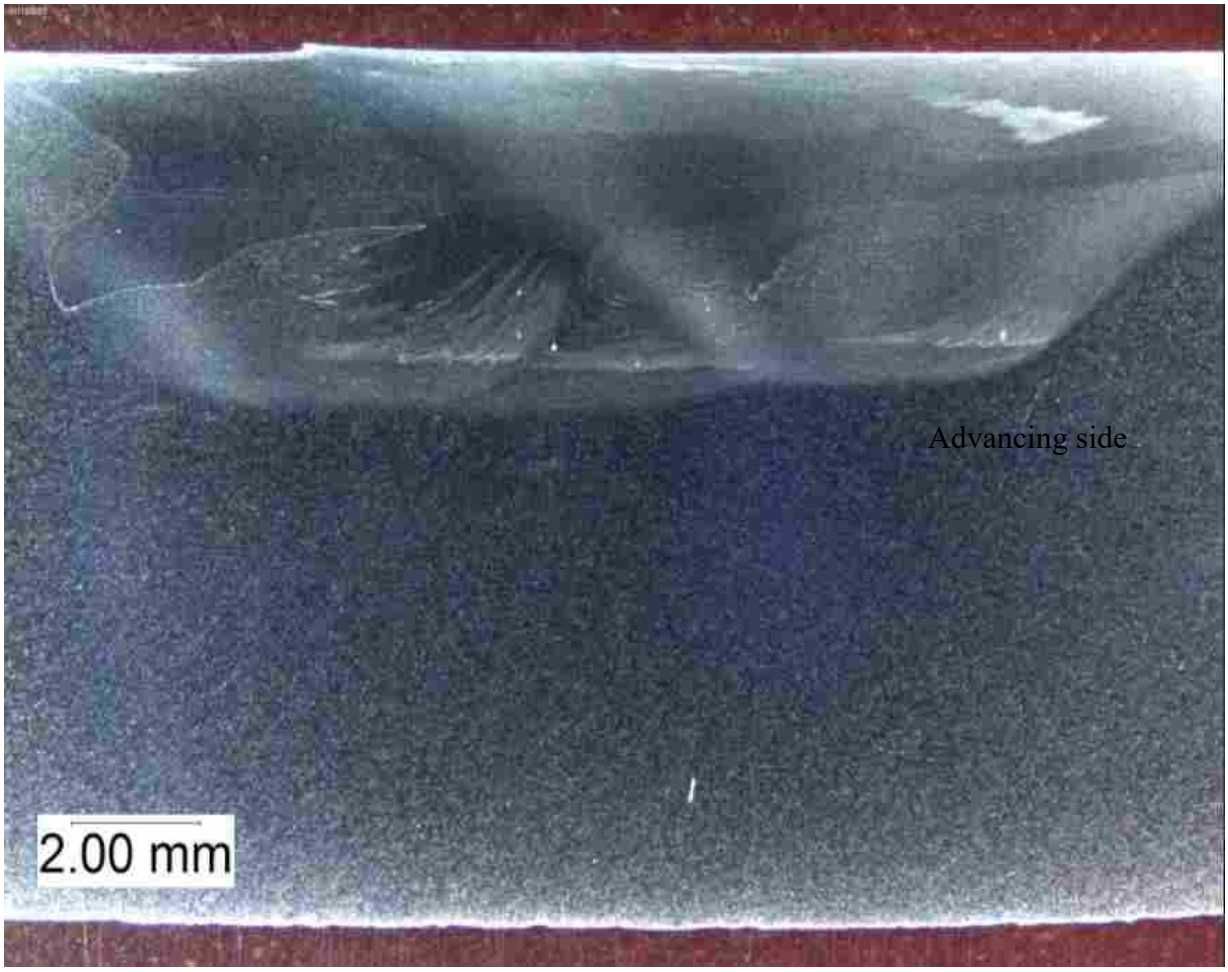

Figure 4-3: 304L Stainless Steel with 0.5” x 0.15” Insert with No Macro or Micro Voids

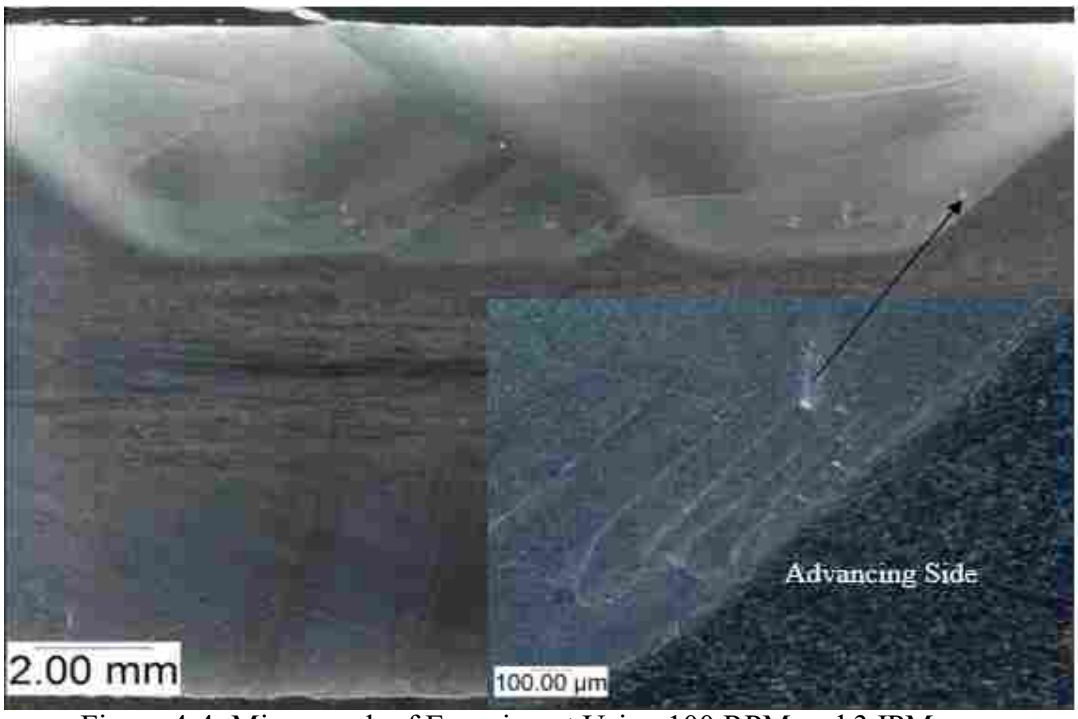

Figure 4-4: Micrograph of Experiment Using 100 RPM and 3 IPM

4.2 Tensile Testing

Tensile testing was used as a standard to measure the effectiveness of the joint in terms of strength. Three dog bones were taken from each plate that had a reduced section that measured a 0.25” wide, 1.25” long, and a 0.25” in thickness. After the dog-bones had been cut and machined, they were placed in bags to sort the individual geometries that the dog-bones came from, and then they were pulled and marked. Results from the first plate were poor because it lacked friction stir processing. The second experiment used friction stir processing showed improvement in tensile strength. However, data from the specimens still showed that strength was poor and in many cases lower than the base material. It seemed that void content was also causing problems in achieving higher strength. In order to achieve more favorable results in microscopy and tensile strength, geometries were changed to reflect a ball nose end mill machined cross section. Results from the third experiment which used the ball nose end mill

showed substantially improved strengths, in some cases up to twenty percent over the BM. Each section that the three dog-bones were taken yielded consistent results. For the third experiment a design of experiments (DOE) was also in place to randomize the specimens to see if there was any correlation with the process parameters. Specifically, depth of the geometries, and width. The data from the third experiment when placed under statistical analysis showed a linear correlation relating to the depth. It showed that as depth increases, tensile strength decreases which can be seen if figure 4-5. However, because all tensile specimens were machined to the same depth from the back side of the plate the data should have been consistent. This was most likely due to the fact that with deeper geometries, more heat entered the material during the MIG filling process. Therefore, there was a larger area affected by the heat going into the material which may have remained after FSP. In addition, using MIG welding as the additive process proved difficult to eliminate voids if the same settings were used for all geometries. The deeper a machined pocket would go; the more likely voids would appear. This is most likely due to how the MIG weld cooled in the deeper slots. Even with the switch to using ball nose tooling, the same trend occurred. Elongation data which can be seen in figure 4-6 revealed that MIG filled areas did not give us the consistency we needed for this to be a valuable process. Elongation would often correlate with UTS data because if the sample did not fail early because of voids then it could elongate further and achieve a higher UTS.

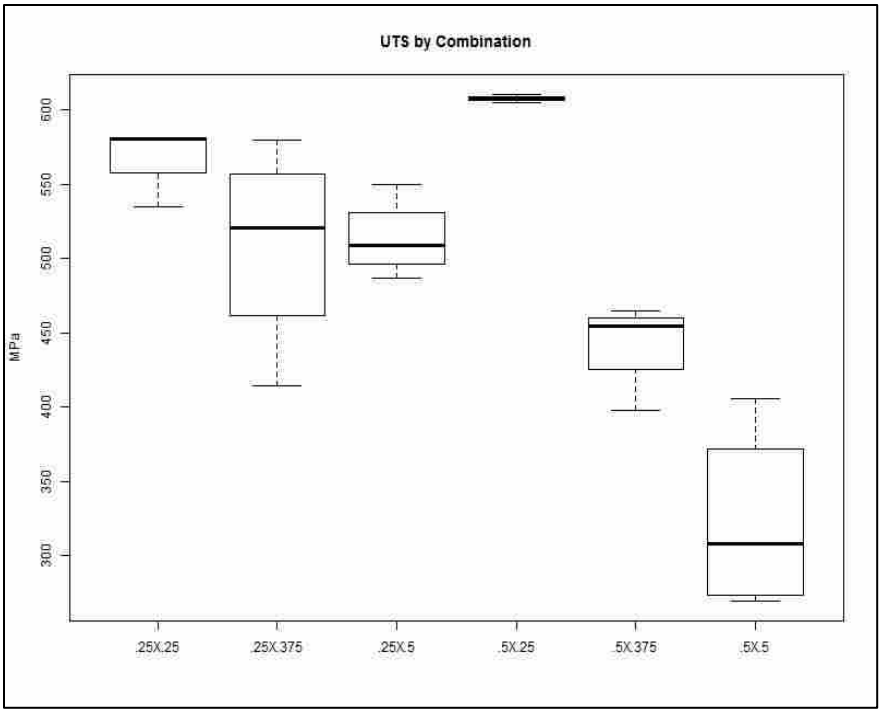

Figure 4-5: UTS Strength Against Geometries

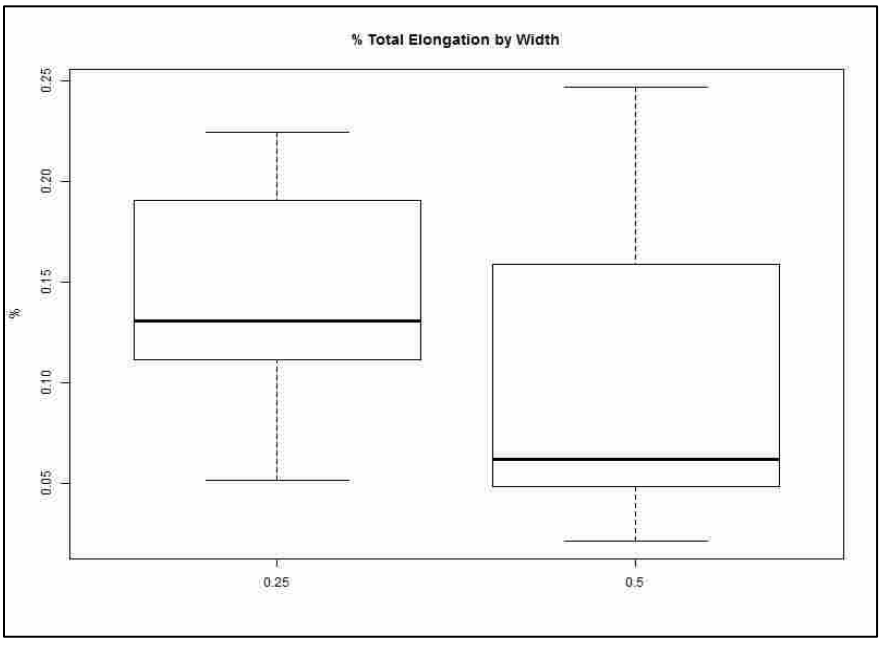

Figure 4-6: Elongation by Width of MIG-Filled Section

Another problem that had to be resolved was significant distortion of plates after welding and FSP. All plates showed bowing of both sides down the length of the plate which can be seen in figure 4-7 from a specimen that was cut. Also after the plate had been MIG welded, the warping made it very difficult to process and machine to prepare for FSP. After the FSP, additional warping was observed. In some cases, some specimens could not be machined because of the substantial warping which can be seen in figure 4-7. These specimens were not usable because machining would have removed too much material to get accurate data. Because each plate was 0.75" thick some thought was given to pre-heating the plate to reduce the warping. However, this seemed like a more expensive and time consuming process. It also became clear the warping made MIG impractical for this process. This is because filling in the inserts with MIG welding took more time and depending on the depth it took a greater amount of energy and heat that could warp the plate further. Pre stressing the plate to prevent warping was not done because in some field applications where this process could be used, pre-stressing may not be possible.

Figure 4-7: Specimen That Could Not Be Processed Because of Warping

It was decided that instead of using MIG welding as the process to add material, to create inserts that would be placed into the slots. This is because an insert could be machined in less time and reduced the overall process time by at least 50 percent. Some plates took over an hour to fill in the slots by MIG welding. Yet an insert could be made in 15 minutes and be placed into the slot. Once the insert was placed no additional facing was required and no warping was observed. A plate was prepared for the fourth experiment and the number of slots was reduced to two. Because of the linear correlation that was observed in the DOE it was decided that we would not have a depth below 0.25". However, two different widths were still being used which were .25 inches and .5 inches. The inserts were machined out the same material as the plate to be FSP. Each insert was 0.2" thick and was 0.001 larger than slot. The inserts were then press fit in and then the plate was processed. No warping was observed and much more desirable results for processing were achieved.

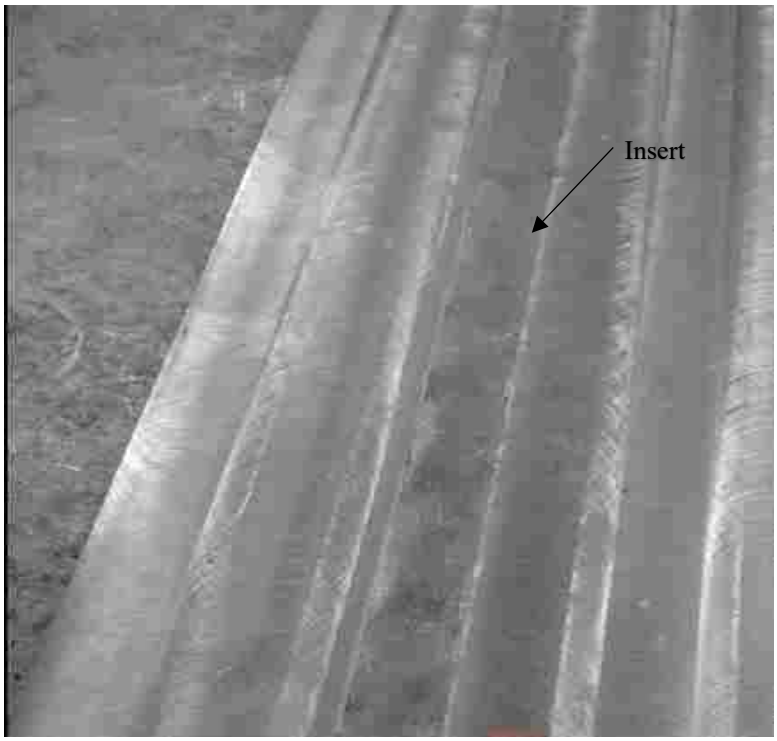

Figure 4-8: Plate with Machined Inserts

The plate with the insert before processing can be seen in figure 4-8. While a press fit was used for this experiment, eventually inserts were machined to size. This was because it turned out the force from the FSP tool would ensure that there were no gaps between the insert wall and slot wall. The z force coming from the tool forced the insert to spread to the wall of the slot. This made placing the inserts easier because freezing the insert and preheating the plate became unnecessary. After the plate underwent FSP, tensile strength data showed some improvement over the ball-nose end mill experiment.

With the success of the insert experiment in mild steel, the same parameters were used in the following stainless steel experiments. However stainless proved to be more difficult to achieve a successful weld than 1018 mild steel. During FSP the inserts would bow outward because of the force from the tool. Because of this the inserts were tack welded down in place with TIG spot welds. Additionally, running the same parameters were abrasive on the tool to the point where in one experiment the tool shattered. It was determined the tool was plunging too deep. In later experiments a new slot depth was used to prevent the tool from plunging so deep. The new slot depth that was chosen was 0.15”. This depth was chosen because a safe tool depth would be 0.18” which was used in previous experiments (Gunter, 2016) and it would allow the tool to pass underneath the insert to ensure complete blending. On analyzing cross sections of the welds, blending did occur as it had done in the mild steel experiments but a small void was seen near the edge of the pin on the advancing side. Tensile strength was higher than the mild steel which can be seen in table 1 and 2. Figure 4-9 shows tensile data before parameters were adjusted. This showed better performance for a narrower insert rather than a wider insert like the 1018 showed. This may have occurred in stainless steel for a variety of reasons. No tilt was used during this experiment and a deeper depth was used. It might be possible that mild steel can blend easier

than stainless steel and so a wider geometry would be more difficult to achieve complete homogenous blending. However, voids in the cross section still occurred which can be seen in previously shown figure 3-4.

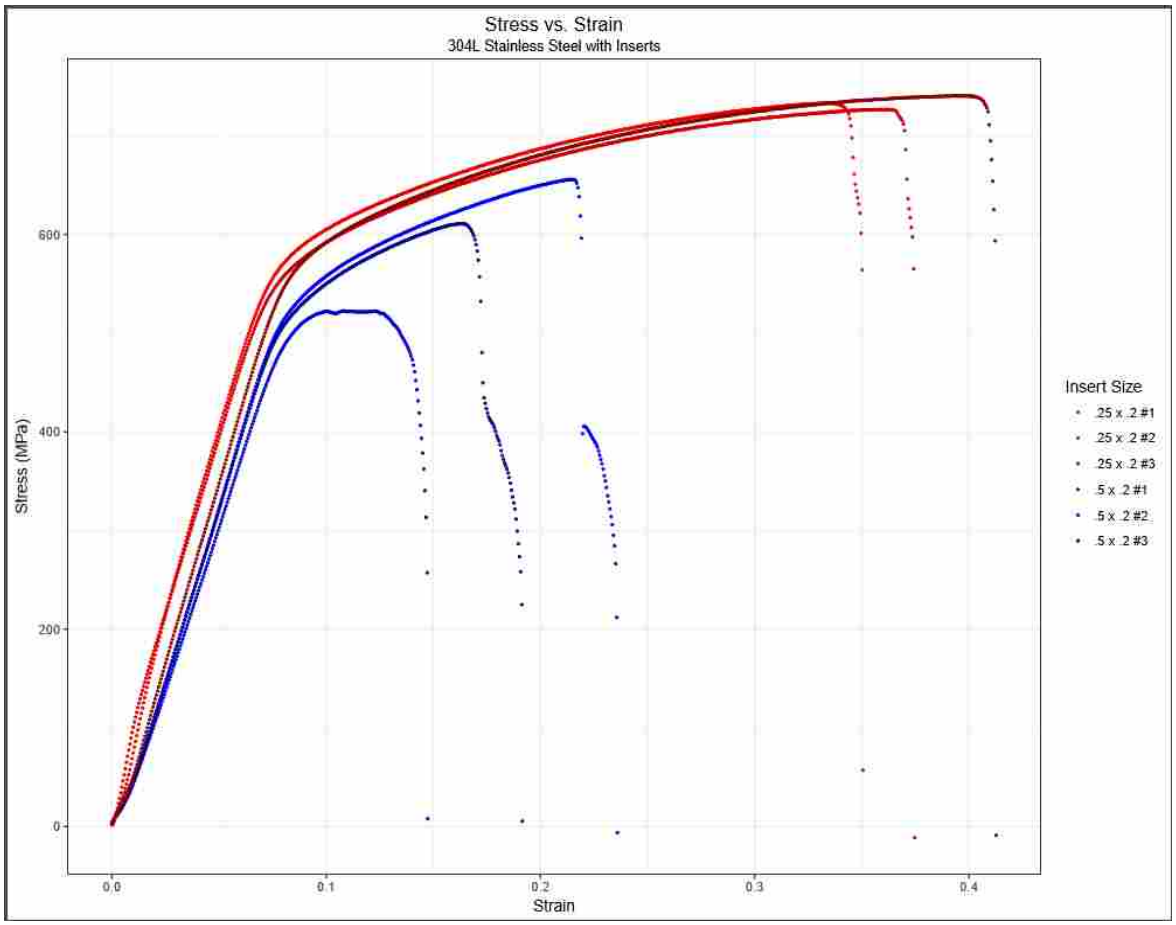

Figure 4-9: Stainless Steel Tensile Results Before FSP Parameters Were Adjusted

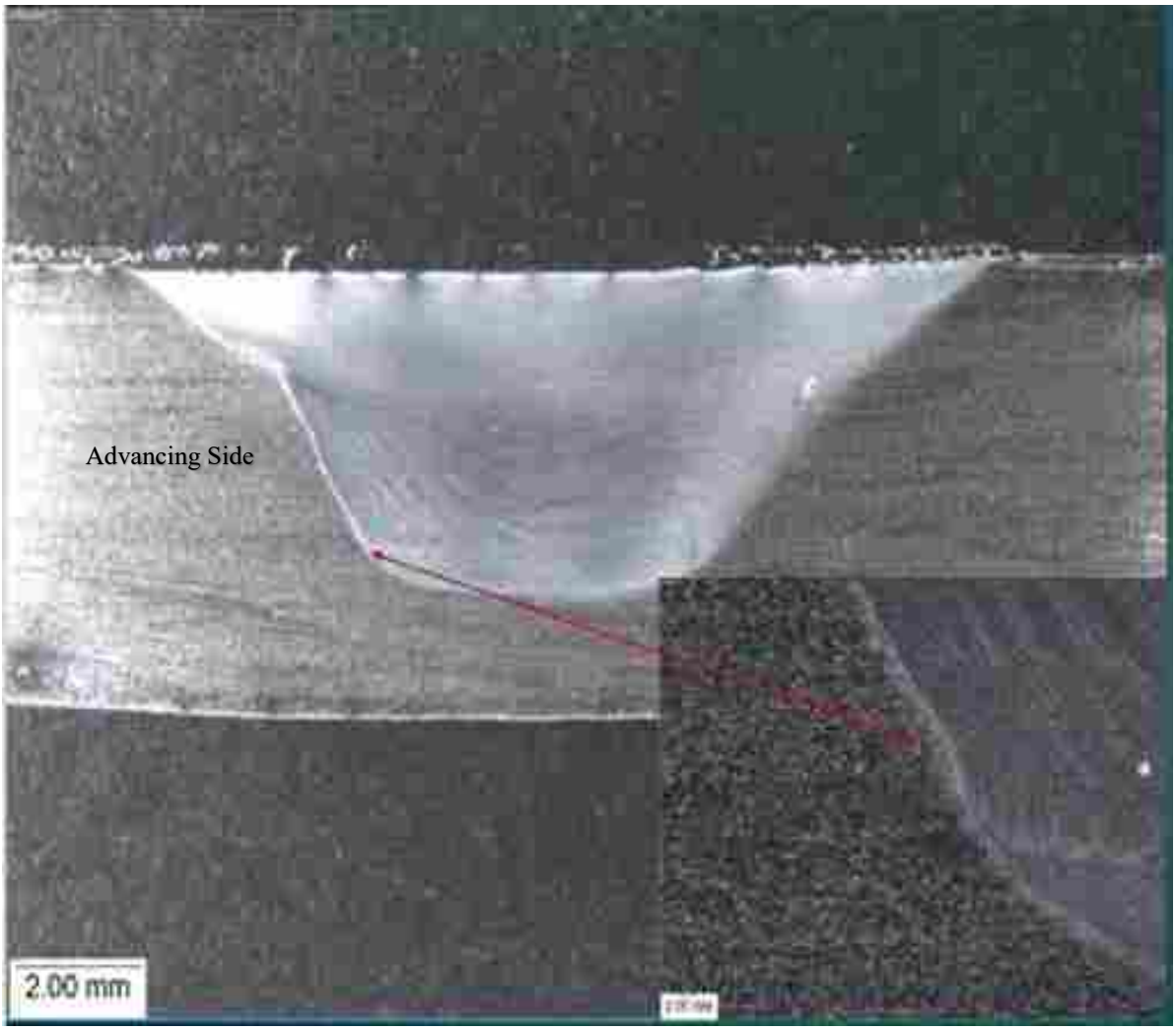

Figure 4-10: 200RPM and 3IPM 1 FSP Pass Sample with No Voids

4.2.1 Parameter Adjustments and Void Reduction

Before another experiment with inserts was processed, proper parameters for stainless steel were needed. Three different parameters were tried and it was decided based on weld appearance and microscopy data that 200 RPM and 3 IPM would be used. The first experiment to use the decided parameters had three plates that each had one insert. Each insert was 0.5” X 10” X 0.15” and placed six inches from one end of the plate where the tool would plunge. The FSP pass order was varied to see if it had any effect on consolidation. Each plate showed defects and wormholes or tunnel defects because of lack of pressure and due to the order of the weld passes. Microscopy revealed that when starting the first path in the middle, the z force deformed the insert and increased the width of the insert until both sides of the insert were hitting the slot walls. This effect can be seen in figure 4-12. This prevented any opening between the insert and slot wall that could not be closed. An experiment was run with running the first pass down the center and microscopy showed reduced voids and sizes and it showed compression between the insert and slot wall. The diagram seen in figure 4-11 illustrates the friction stir process paths chosen. The first plate started with the first path down on the right side and a second pass down the center and the final pass down the left side. The second plate was processed the same as the previous experiments. The third plate was processed with the first pass on the left, second pass down the middle and the final pass on the right.

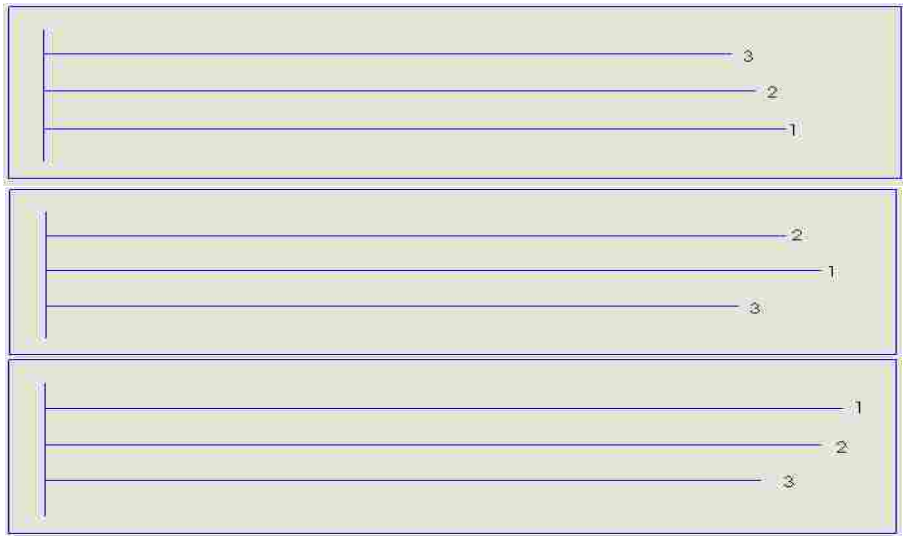

Figure 4-11: FSP Pass Order for Plate 1,2, and 3

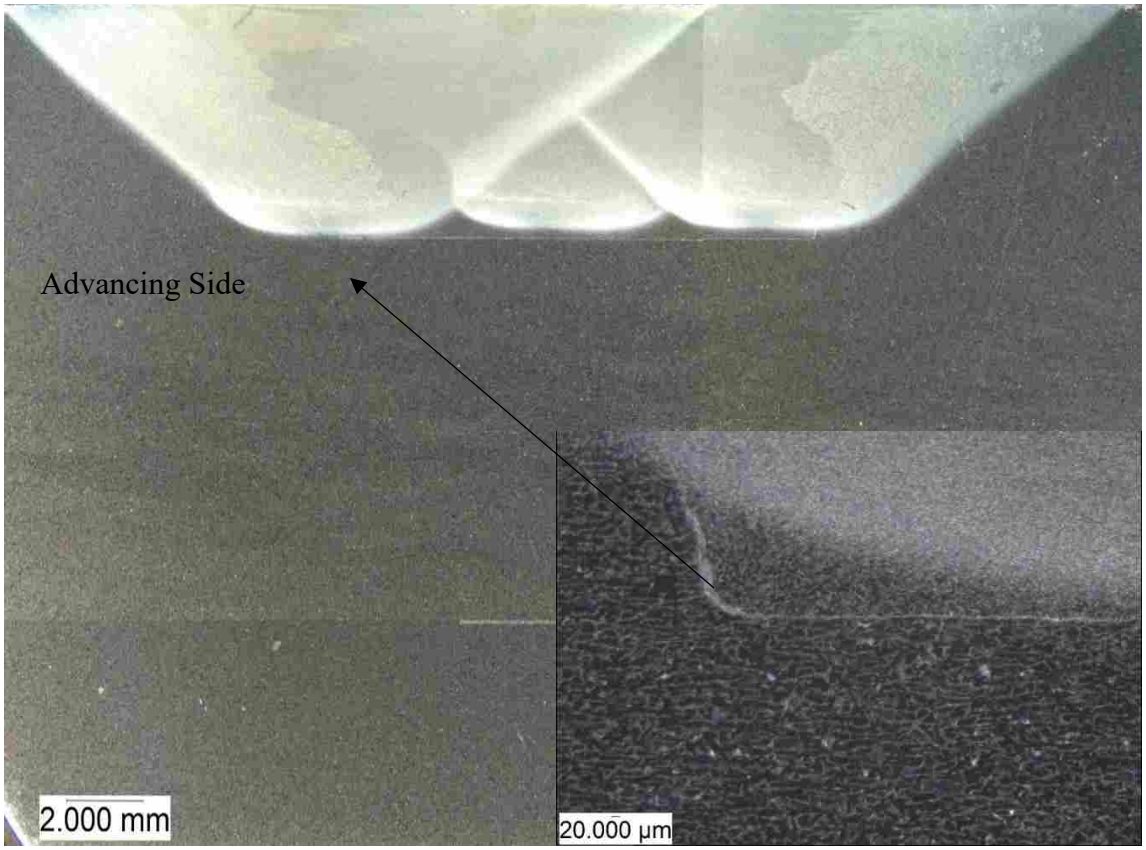

Figure 4-12: 1018 Steel Micrograph Showing Insert Expansion After FSP

Micro voids which can be seen in figure 4-16, were still observed because the experiment was run without any backward tilt on the tool. Microscopic examination also showed a correlation between temperature and large voids or tunnel defects. For example, for many experiments, once the tool temperature exceeded 800° C large voids would open on the advancing side of the SZ. The next experiment had parameters changed so the temperature would not go above 800° C. While most of the large voids disappeared, the micro voids at the bottom of the pin on the advancing side were still visible as can be seen in figure 4-16. This figure shows and a weld with close up images on the left taken at 22X and the bottom right taken at 90X. It was then thought that some of the voids were possibly occurring because during these experiments the tool had 0° tilt. Although a tapered tool is often run with a 0° tilt in some cases a slight backward tilt angle has been shown to reduce voids and improve SZ consolidation. Another measure taken to prevent voids was to regrind the tool. The data that was gained from several experiments in stainless steel that had voids did not help identify what was causing the voids completely. This was because when and where the voids occurred was not consistent. Although identifying a max temperature was helpful, even that was only consistent 9 out of 12 passes. Before the next experiment, the tool was reviewed and found to have threads that were worn. Worn threads do not allow the tool to be as effective. This is because worn threads do not give additional downward force to push material into the needed areas such as at the bottom of the pin on the advancing side. Once the tool was reground, two plates were prepared with inserts and were processed using parameters of 200 RPM and 3IPM for one plate and 150 RPM and 3 IPM for the other. The change in RPM was to help control the temperature and keep it below 800° C because of previous experiments, reviewing tool, and microscopy data showed that FSP above 800° C shortened tool life and increased the possibility of macro voids appearing. Once

tensile specimens were cut, they were taken from the plate with 200 RPM and 3 IPM. FSP in these plates did not improve tensile strength over the base material. This was because a non-volumetric defect was in the SZ. However, the specimens that came from a plate using 150 RPM and 3 IPM had improved tensile strength over the base material. This confirmed the previous works conclusion that a lower RPM had an effect in increasing tensile strength (Gunter 2016). Because both sets of specimens came from a SZ that used 3 IPM, a lower RPM would allow FSP at a lower temperature if z force was also the same. In this experiment temperature was controlled by running a constant z force of 10000 pounds on one plate and 8000 pounds on the other. The plate with 10000 pounds of z force had higher temperatures and so the RPM was adjusted to 150. This lowered the temperature of the SZ below 800 C. When the plate with 8000 pounds of z force was being processed no adjustment was made. Temperatures stayed at around 800° C. Elongation in these specimens did show a decrease which may be due to a larger SZ created by three FSP passes. This may be due to lower temperatures during FSP which would lead to less grain growth. However, because similar parameters were done in previous supporting work, the higher UTS could be due to the Hall-Petch effect. This can be seen in previous work that shows a smaller grain size increasing hardness in FSP specimens (Gunter, 2016). With a hardened SZ, there was less material that could elongate especially when three passes were done. This was clearly evident with the increase in number of FSP passes where there was a much larger area around the SZ that was hardened because of grain refinement and because of the heat coming from each subsequent pass. Because of the non-volumetric defect that occurred in the SZ, another experiment was conducted with parameters of 100 RPM and 3IPM and with a z force of 12500 pounds and 1-degree tilt. This was done because previous data using these parameters on stainless steel showed high tensile strength and elongation. However, it did not

achieve consolidation which was previously shown in figure 3-4. It was thought that the defect possibly occurred because that previous experiment was run with 0-degree tilt. The results showed much higher tensile strength and elongation. Failure in tensile specimens occurred in the base material instead of the SZ which are shown in figure 4-13. The failure occurred away from the retreating side in the BM. Max ultimate tensile strengths and elongation can be seen in tables 1 and 2 below. In figures 14 and 15, a graphical representation of the max UTS and % elongation can also be seen showing that 100 RPM and 3 IPM gave the best results when compared to other FSP parameters. UTS on the geometry of 0.5" X 0.15" was significantly better than 0.5" X 0.2".

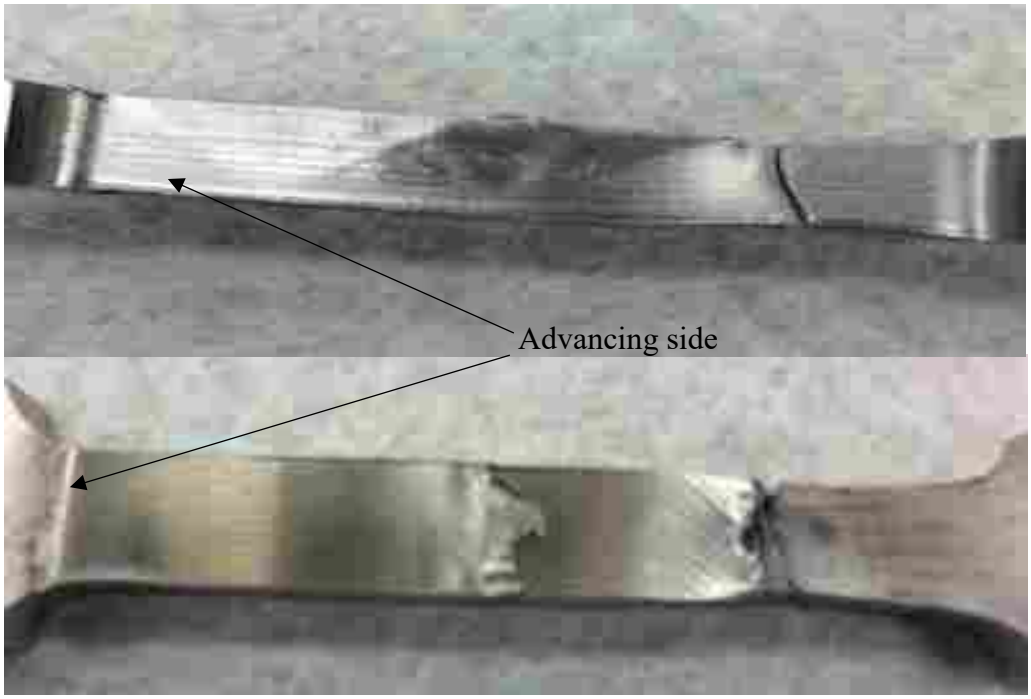

Figure 4-13: Tensile Specimens with FSP Parameters 100 RPM and 3 IPM

Table 1: Max UTS and Elongation for 1018 steel

Material/ Geometry	Base Material	.5X.25 MIG WELD	.5X.25 MIG and SZ	.5X.25 Ball nose MIG and SZ	.5X.2 Insert And SZ
UTS	516 MPa	242 MPa	312 MPa	610 MPa	619 MPa
elongation	34%	5%	1.2%	31%	25%
FSP Parameters	N/A	N/A	100 RPM 3 IPM	100 RPM 3 IPM	100 RPM 3 IPM

Table 2: Max UTS and Elongation for 304L

Material & Geometry	Base Material	.5X.2 Insert	.25X.2 Insert	1 pass	5X.15 Insert	.5X.15 Insert	.5X.15 Insert
UTS	610 MPa	655 MPa	740 MPa	639 MPa	603 MPa	633 MPa	730 MPa
Elongation	71%	21%	40%	50%	18%	22%	38%
FSP Parameters	N/A	100 RPM 3 IPM	100 RPM 3 IPM	200 RPM 3 IPM	200 RPM 3 IPM	150 RPM 3 IPM	100 RPM 3IPM

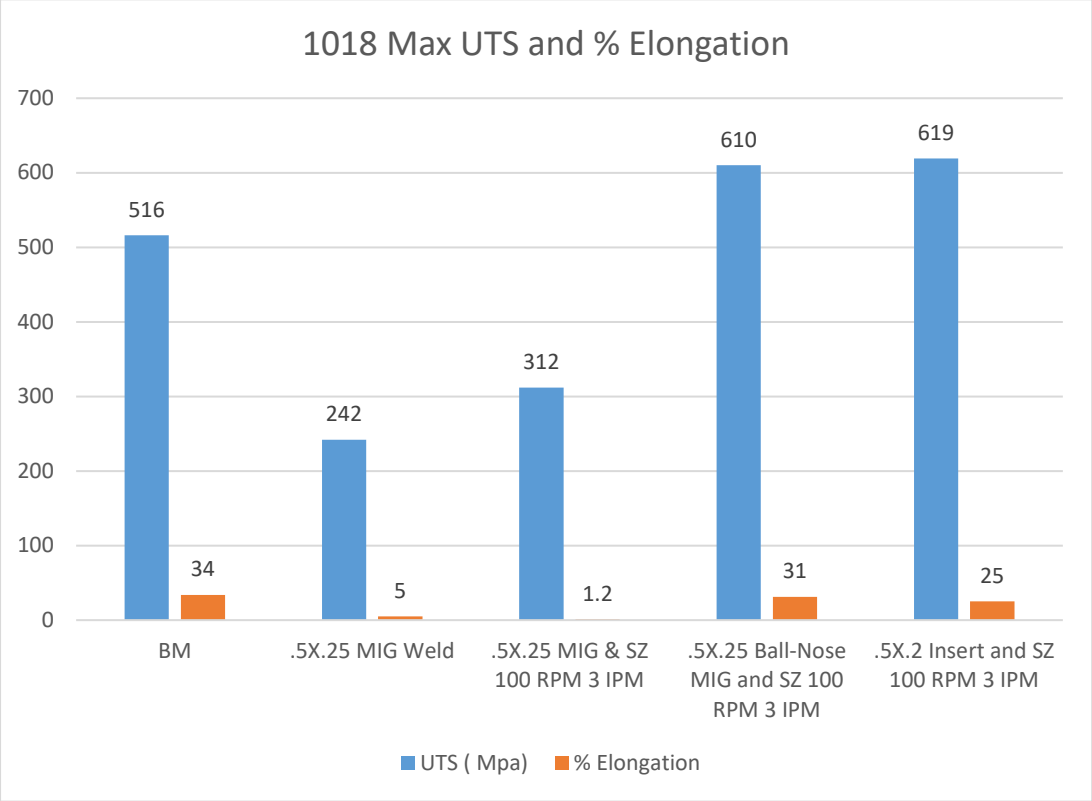

Figure 4-14: Graphical Representation of 1018 UTS and % Elongation

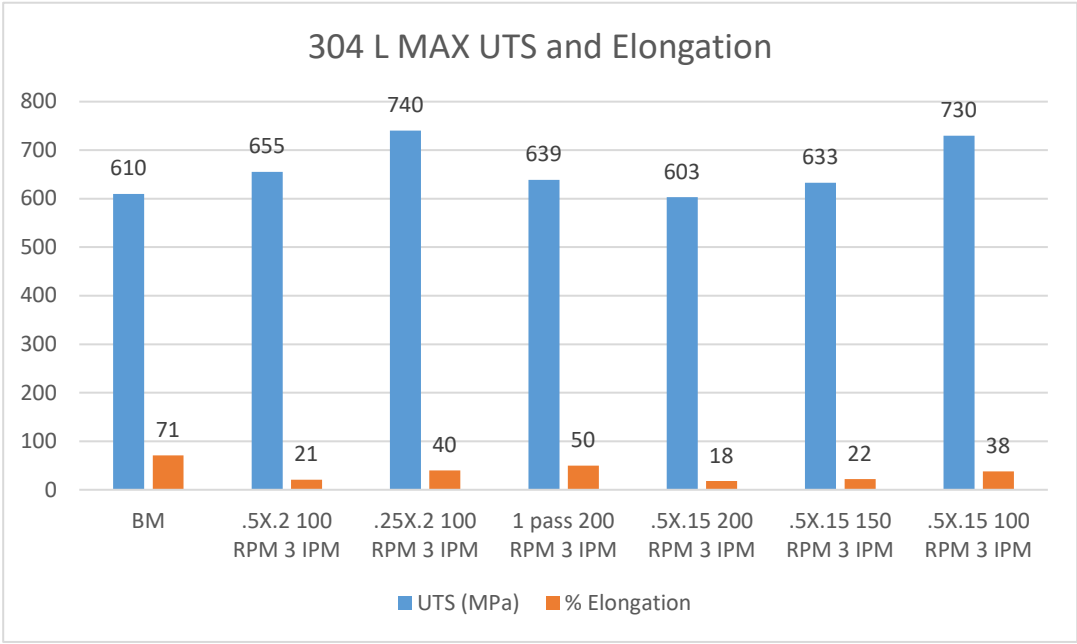

Figure 4-15: Graphical Representation of 304L UTS and % Elongation

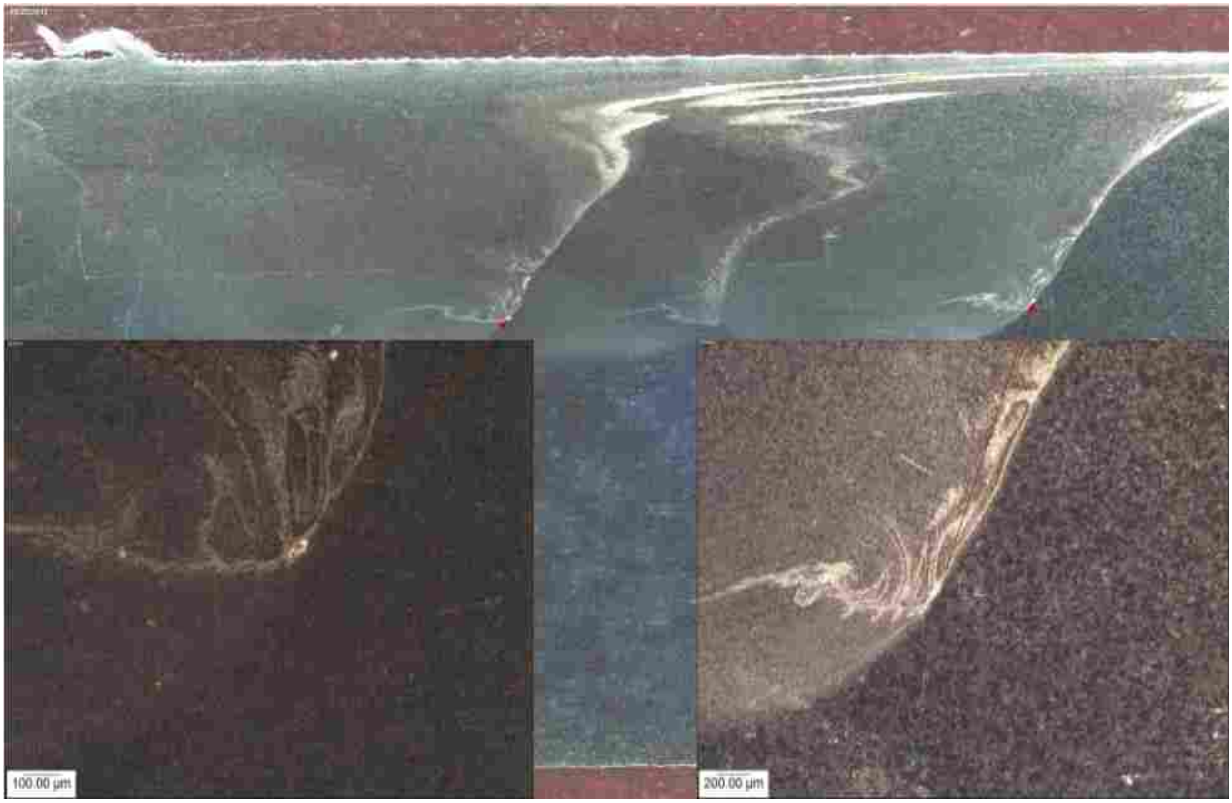

Figure 4-16: Stainless Steel with Insert Showing Micro Voids

4.3 Micro-Hardness Mapping

Because in initial experiments poor tensile strength was observed, micro hardness mapping was done to gather more information in hope to gain more understanding of what was causing poor results. Micro hardness mapping was done using a diamond micro hardness tool with 400-micron spacing. Most samples because of their size took three days to gather all the data. One sample was taken from a plate with a single pass and another from a plate with three passes. Each had the same geometry which was 0.25” wide and 0.375” deep. This geometry was chosen because it had excellent microscopy images when compared to the other specimens. With the ball nose experiment, the sample with the lowest strength was used to see if there were any indicators or abnormalities that would help explain the poor tensile results in geometries that

were deeper. Hardness mapping showed that if MIG was used then the weld nugget would be softer after FSP. This can be seen in figures 4-15 and 4-16. However, the SZ was still observed to be harder than the base material with a heat affected zone. Figures 4-16 and 4-17 show an increase in area that had been hardened. This could be because these welds had three FSP passes instead of one and so the steel specimen retained heat from each pass.

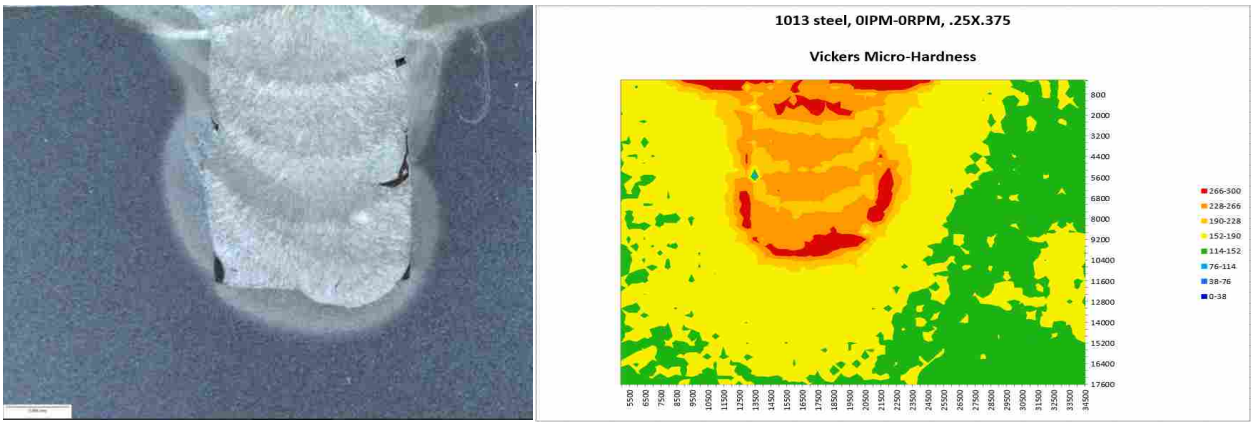

Figure 4-17: Hardness Map of Un-Processed Weld

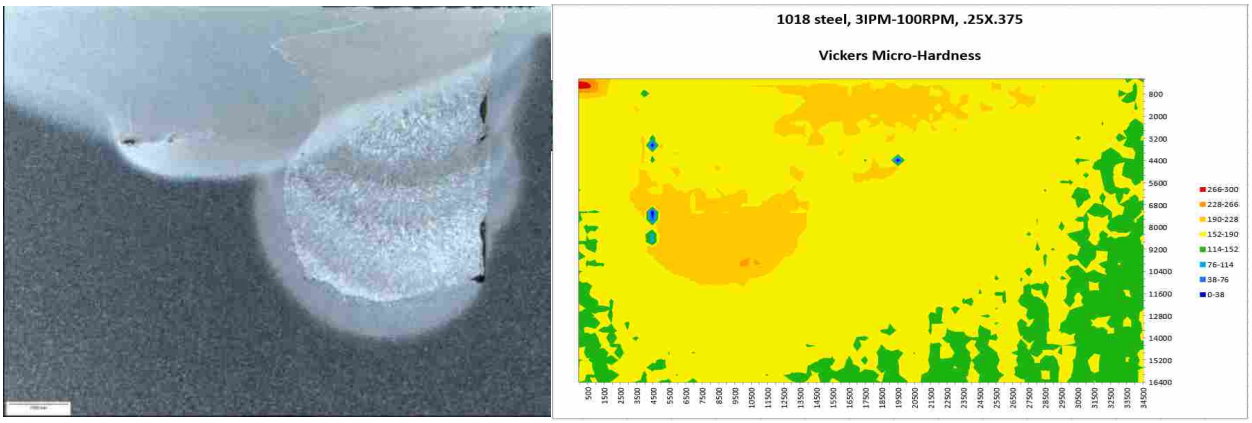

Figure 4-18: Hardness Map of Weld After FSP

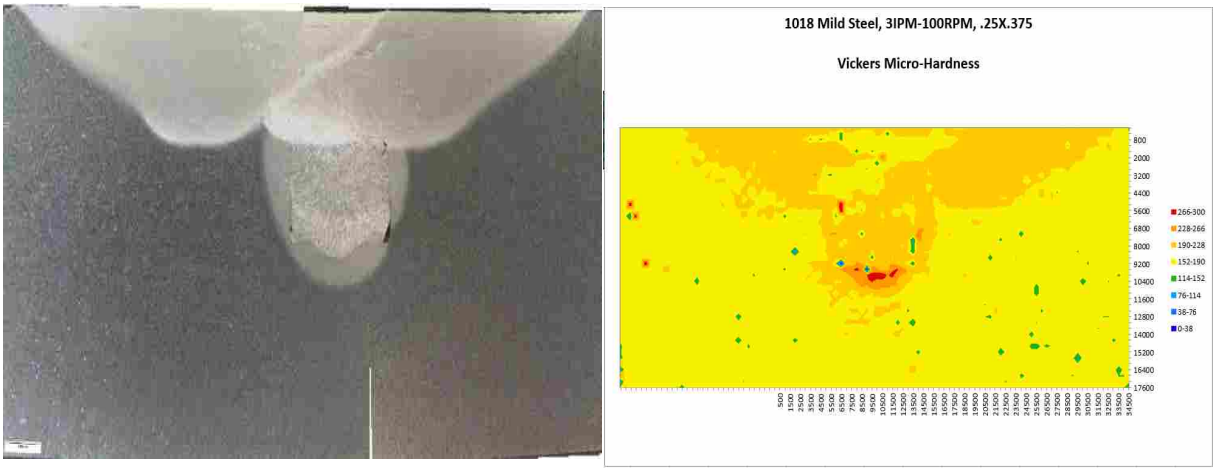

Figure 4-19: Hardness Map of Slot with Square Geometry

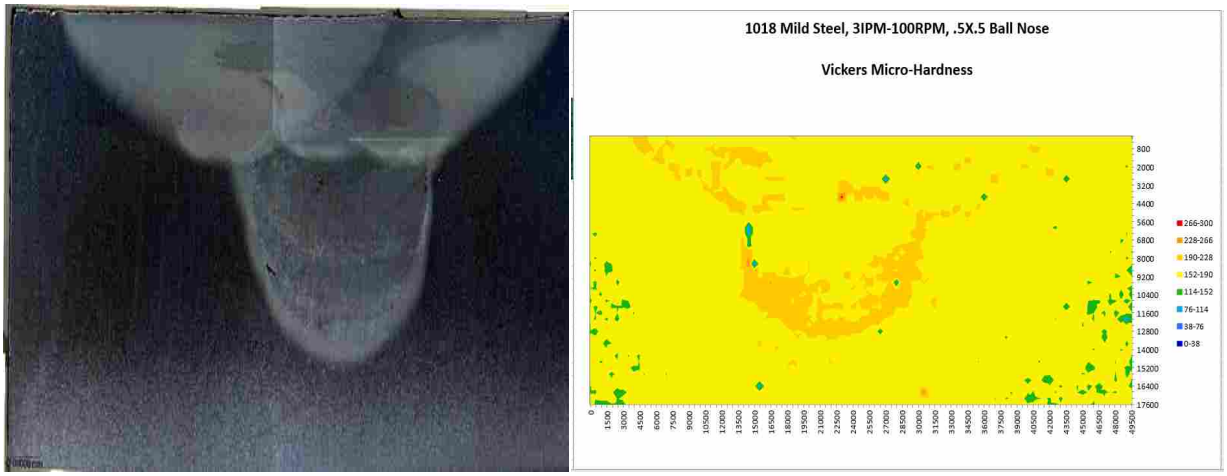

Figure 4-20: Micrograph of .5X.5 Ball Nose Geometry

4.4 Three-Point Bend Testing

Three-point bend samples were cut and prepared in a similar manner when compared to the tensile specimens. Using a band saw, samples were cut according to the ASTM E8 standards which are 4” wide 0.5” thick and 0.5” long (Baratta 1992). The samples were also machined on the sides to meet the tolerance standards. Once the samples were prepared, they were then cut on the wire EDM and then bent. All samples were bent using a three-point fixture that had the top

point descend 0.030” inches per minute until it reached 0.3”. Initial inspection showed crack propagation around the SZ. Rather than propagating through the nugget, the crack would travel around the harder material. This was evident in all FSP samples. In the base material the samples would elastically deform.

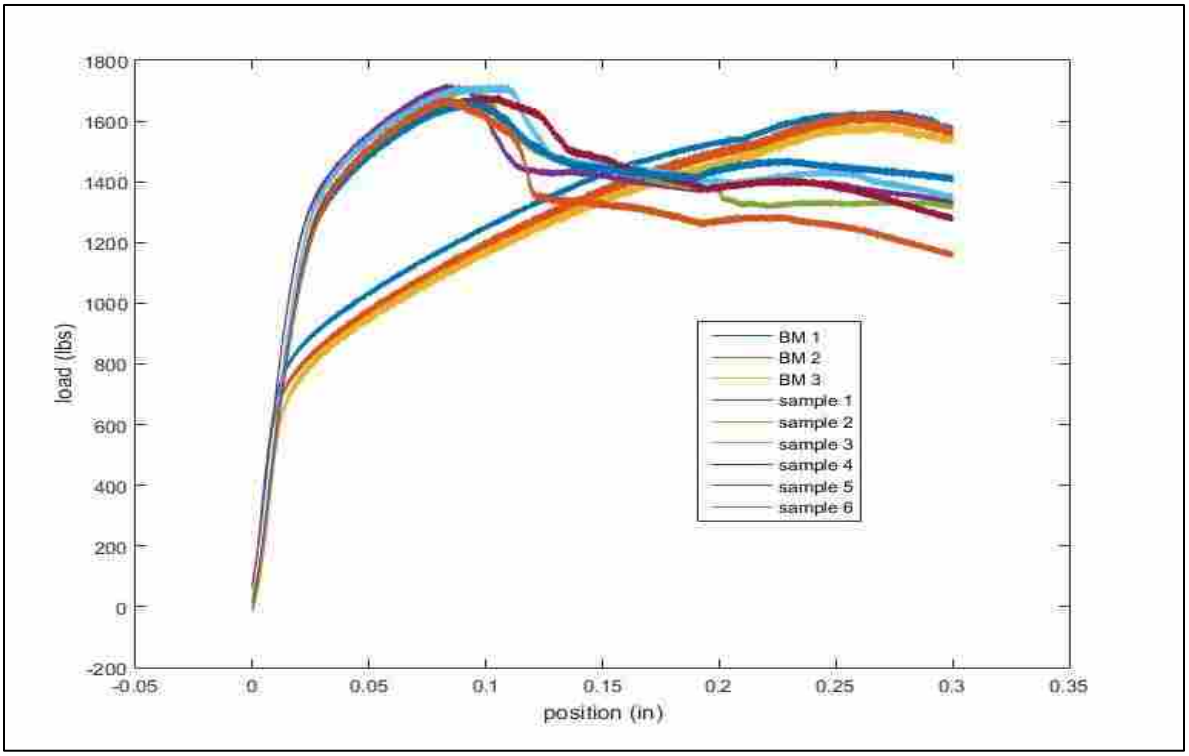

Figure 4-21: Load vs Displacement of Base Material and Welded Material

The base material had a much lower yield strength than specimens that had a SZ in them. The specimens with FSP material also absorbed 10% more energy than the base material before yielding. Figure 4-21 above shows the drastic difference in yield strength based on the initial review of the data. It shows the base material yielding at 700 pounds and the SZ specimens yielding around 1300 pounds.

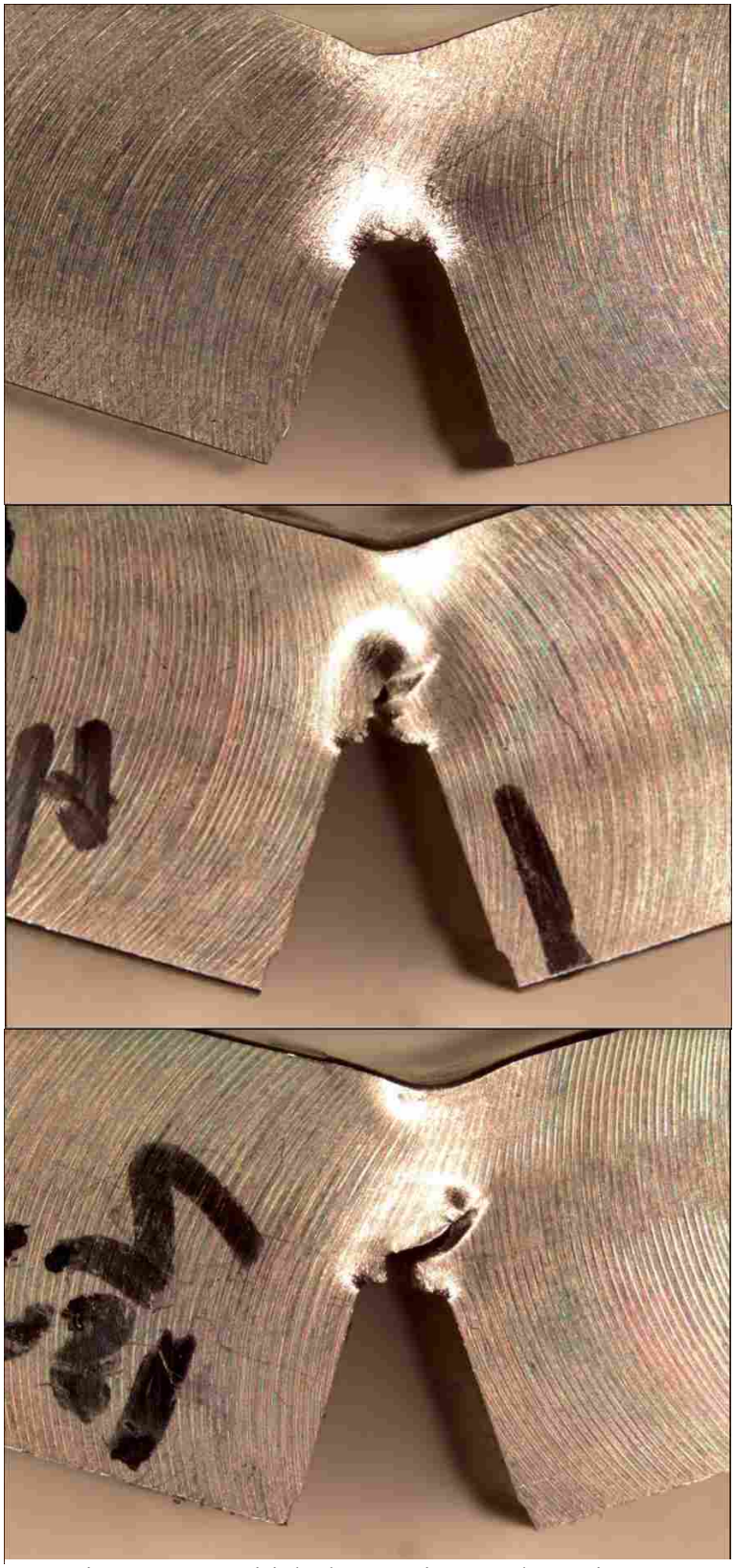

Figure 4-22: Initial Three-Point Bend Specimens

This would also show that this could be effective in stopping internal SCC if the tool is unable to reach the crack at all. The Images of the base material and specimens with a weld nugget can be seen in figure 4-22 and in 4-23. It is seen that in the base material only

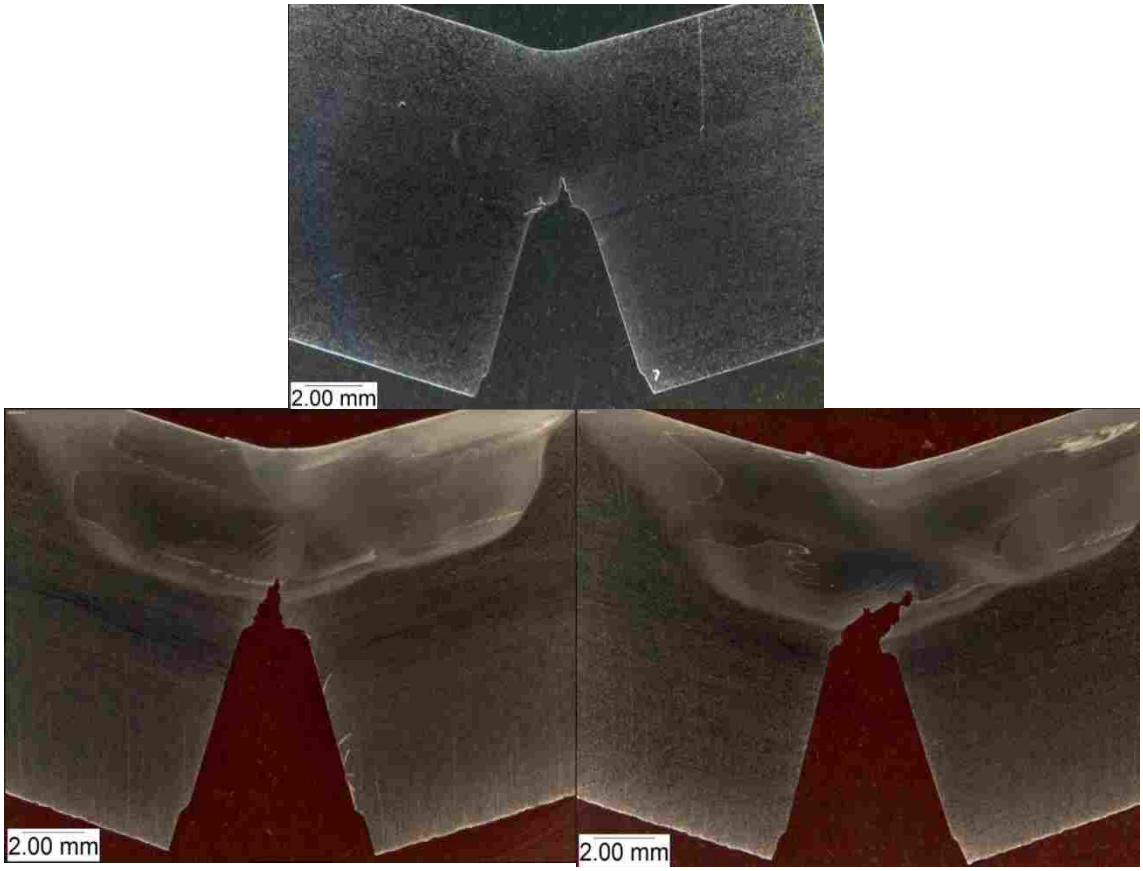

Figure 4-23: Micrographs of Three-Point Bend Specimens

plastic deformation occurs. But with a SZ cracking does occur. With 8000 lbs. of z force and at 200 RPM and 3 IPM the crack went up and blunted and plastic deformation occurred and the crack appeared that it would go off to the right if the experiment went any deeper. With 10,000 lbs. of z force and 150 RPM and 3 IPM the crack did go off to the right to go around the SZ.

5 CONCLUSIONS AND RECOMMENDATIONS

5.1 Additive and FSP Produce a Consolidated Weld.

H1: Using added material into the area needing repair, full weld consolidation will occur using either 100, 150 or 200 RPM and 3IPM on stainless steels and using 100 RPM and 3 IPM on mild steels. Full consolidation was achieved with the exception of an extremely small void on the advancing side of the final pass which can be seen in figure 4-4. Despite this void being there, tensile specimens showed that failure occurred in the base material. When using 100 RPM and 3 IPM on 1018 consolidation would occur. In many cases if there was a slight gap between the wall of the slot and the insert, the z force from the friction stir tool would close the gap and heal the area. Microscopy was valuable in seeing how effective was the process in blending the added material into the base material. Grain refinement occurred in both insert and base material although oxide from the insert still remained. While a small void did occur in SZ, FSP and additional microscopy data shows that this could possibly be eliminated with additional z force on the second or third passes. Micro-hardness mapping also revealed that when using a wire fed additive process, the initial added material is much harder than the base material. When the material has been stirred it softens but still remains harder than the base material. Some additional work that could be done would to see if adding a harder or softer insert changes the effectiveness of the process.

5.2 Tensile Testing

Based on tensile data and graphs seen in figures 4-14 and 4-15, 100 RPM and 3 IPM had the best results. UTS was 20% better than the BM. Elongation was the highest when compared to other specimens with a SZ even though it was 28% less than the BM. The void shown in figure 4-4 had no effect on the UTS or elongation because the specimens failed in the base material rather than the weld nugget. When using 200 RPM and 3 IPM, full consolidation did occur but a non-volumetric defect caused tensile specimens to fail in the SZ. They also showed no increase in tensile strength and had poor elongation. Some specimens had an elongation of 20% which is 70% lower than the BM elongation.

5.3 Three-Point Bend Testing

H2: If an existing crack is beneath the surface it will not propagate through the SZ. The grain refinement created a much harder zone that a crack could not propagate through. Because of this grain refinement, the crack would blunt and change direction rather than propagating through the SZ. Some further work that could be done would be to see if changing the FSP parameters affects crack propagation or if a wire fed additive process would have changed how the crack would have propagated.

REFERENCES

Baratta, F. and J. Underwood (1992). "Notch Dimensions for Three-Point Bend Fracture Specimens Based on Compliance Analyses."

Baufeld, B., et al. (2010). "Additive manufacturing of Ti–6Al–4V components by shaped metal deposition: Microstructure and mechanical properties." Materials & Design 31: S106-S111.

Brandl, E., et al. (2012). "Morphology, microstructure, and hardness of titanium (Ti-6Al-4V) blocks deposited by wire-feed additive layer manufacturing (ALM)." Materials Science and Engineering: A 532: 295-307.

Cheng, C. F. (1975). "Intergranular stress-assisted corrosion cracking of austenitic alloys in water-cooled nuclear reactors." Journal of Nuclear Materials 57(1): 11-33.

Cissé, S., et al. (2012). "Effect of surface preparation on the corrosion of austenitic stainless steel 304L in high temperature steam and simulated PWR primary water." Corrosion Science 56:209-216.

Clocksin, W. F., et al. (1985). "An Implementation of Model-Based Visual Feedback for Robot Arc Welding of Thin Sheet Steel." The International Journal of Robotics Research 4(1): 13-26.

Ding, D., et al. (2015). "Wire-feed additive manufacturing of metal components: technologies, developments and future interests." The International Journal of Advanced Manufacturing Technology 81(1): 465-481.

Fino, P. and L. Iuliano (2013). "Influence of process parameters on surface roughness of aluminum parts produced by DMLS." INTERNATIONAL JOURNAL, ADVANCED MANUFACTURING TECHNOLOGY 67 (Springer Verlag Germany).

Flak, R., et al. (2006). Solid state processing of materials through friction stir processing and friction stir mixing, Google Patents.

Gåård, A., et al. (2006). "Microstructural characterization and wear behavior of (Fe,Ni)–TiC MMC prepared by DMLS." Journal of Alloys and Compounds 421(1): 166-171.

Gibson, B. T., et al. (2014). "Friction stir welding: Process, automation, and control." Journal of Manufacturing Processes 16(1): 56-73.

Grewal, H. S., et al. (2014). "Improving Erosion Resistance of Hydroturbine Steel Using Friction Stir Processing." Journal of Tribology 136(4): 041102-041102-041110.

Gunter, C. C. (2016). Feasibility of friction stir processing (FSP) as a method of healing cracks in irradiated 304L stainless steel.

Corrosion testing was performed with a 1000-hour alternate immersion test in a room temperature 3.5% NaCl solution. With these testing parameters, the results demonstrated that FSP had no effect on the corrosion resistance of 304L SS under these conditions.

Lin, H. T., et al. (1990). "Cavity microstructure and kinetics during gas tungsten arc welding of helium-containing stainless steel." Metallurgical Transactions A 21(9): 2585-2596.

Liu, Q., et al. (2013). "Microstructure and mechanical property of multi-walled carbon nanotubes reinforced aluminum matrix composites fabricated by friction stir processing." Materials & Design 45: 343-348.

Mahmoud, E. R. I., et al. (2010). "Wear characteristics of surface-hybrid-MMCs layer fabricated on aluminum plate by friction stir processing." Wear 268(9): 1111-1121.

Mishra, R. S., et al. (2003). "Friction stir processing: a novel technique for fabrication of surface composite." Materials Science and Engineering: A 341(1): 307-310.

Nagaoka, T., et al. (2015). "Friction stir processing of a D2 tool steel layer fabricated by laser cladding." Materials & Design 83: 224-229.

Palanivel, S., et al. (2015). "Friction stir additive manufacturing for high structural performance through microstructural control in an Mg based WE43 alloy." Materials & Design (1980-2015) 65: 934-952.

Park, S. H. C., et al. (2003). "Rapid formation of the sigma phase in 304 stainless steel during friction stir welding." Scripta Materialia 49(12): 1175-1180.

Razmpoosh, M. H., et al. (2015). "The Grain Structure and Phase Transformations of TWIP Steel During Friction Stir Processing." Journal of Materials Engineering and Performance 24(7): 2826-2835.

Reynolds, A. P., et al. (2003). "Structure, properties, and residual stress of 304L stainless steel friction stir welds." Scripta Materialia 48(9): 1289-1294.

Sorensen, C. D. and T. W. Nelson (2007). "Friction stir welding of ferrous and nickel alloys." Friction stir welding and processing: 111-121.